Dienel and Lauritzen
Fluids and Barriers of the CNS (2025) 22:44
https://doi.org/10.1186/s12987-025-00647-8

Fluids and Barriers of the CNS

REVIEW

Open Access

A budget for brain metabolic water production by glucose catabolism during rest, rises in activity and sleep

Gerald A. Dienel[1,2*] and Martin Lauritzen[3*]

Abstract

Maintaining brain fluid homeostasis is of critical importance for creating a stable environment conducive to optimal neuronal functioning, nutrient distribution, and waste product removal. In this study, we employed previously published data on brain oxygen and glucose consumption in awake rodents or humans to quantify the metabolic water production associated with distinct pathways of glucose metabolism. It is predicted that neuronal mitochondria are the primary source of metabolic water at rest, resulting in a continuous efflux into the cytosol, interstitial fluid, and cerebrospinal fluid. Net metabolic water production is predicted to be reduced by increases in activity due to a shift in metabolism from glucose oxidation to include glycolysis in neurons and ATP hydrolysis by the major cation pumps, which involves water consumption ($ATP + H_2O \rightarrow ADP + Pi$). In comparison, glycogenolysis, which occurs concurrently with the activation of astrocytes, potentially represents a major but previously unidentified contributor to metabolic water. Metabolic water production is dependent on the state of the brain, with a reduction of 30–40% occurring during deep sleep. Our estimates indicate that metabolic water functions as a conduit for interstitial fluid production within the brain, enabling flexible and efficient distribution of fluid that flows seamlessly from the parenchyma to the subarachnoid space and lymphatic vessels to facilitate the removal of brain waste, independent of the glymphatic system.

Keywords Astrocyte, Glucose oxidation, Mechanistic stoichiometry, Mitochondria, Neuron, Perivascular-lymphatic fluid flow

Background

Brain fluids are tightly regulated to provide a stable environment for neuronal function and of great interest because fluid flow is an integral part of normal brain function and a crucial element of distribution of nutrients and clearance of waste products. The blood–brain barrier (BBB) exhibits a low hydraulic conductivity, defined as the volume of fluid that will traverse the barrier per unit time by filtration due to an increase in hydrostatic pressure. This is attributed to the absence of aquaporins in brain endothelial cells [1, 2]. However, water may flow from blood to the brain and vice versa along the endothelial membranes between cells due to osmotic forces produced by the inability of small and large solutes to cross the tight junctions between endothelial cells. Thus, the influx and efflux of water across brain endothelial cells and via solute transporters across the choroid plexus to cerebrospinal fluid (CSF) (see Sects. "Metabolic water

*Correspondence:
Gerald A. Dienel
gadienel@uams.edu
Martin Lauritzen
mlauritz@sund.ku.dk
[1] Department of Neurology, University of Arkansas for Medical Sciences, Little Rock, AR, USA
[2] Department of Cell Biology and Physiology, University of New Mexico School of Medicine, Albuquerque, NM, USA
[3] Department of Neuroscience, University of Copenhagen, Copenhagen, Denmark

© The Author(s) 2025. **Open Access** This article is licensed under a Creative Commons Attribution-NonCommercial-NoDerivatives 4.0 International License, which permits any non-commercial use, sharing, distribution and reproduction in any medium or format, as long as you give appropriate credit to the original author(s) and the source, provide a link to the Creative Commons licence, and indicate if you modified the licensed material. You do not have permission under this licence to share adapted material derived from this article or parts of it. The images or other third party material in this article are included in the article's Creative Commons licence, unless indicated otherwise in a credit line to the material. If material is not included in the article's Creative Commons licence and your intended use is not permitted by statutory regulation or exceeds the permitted use, you will need to obtain permission directly from the copyright holder. To view a copy of this licence, visit http://creativecommons.org/licenses/by-nc-nd/4.0/.

from other substrates and routes" and "Alternative substrates and routes for water fluxes associated with metabolism") is a complex process that is tightly regulated.

Brain cells are separated by the interstitial fluid (ISF), commonly called extracellular space (ECS), that constitutes about 20% of the total brain volume [3]. The ISF space may be characterized as a mesh of fluid-filled "pores" with a width of 38–64 nm, large enough to allow for diffusion of nutrients, metabolites, neurotransmitters, and macromolecules up to the size of immunoglobulin [4], but hardly of sufficient size to allow for bulk flow of ISF-CSF [5]. The recent description of the glymphatic system and of dural lymphatic structures has generated considerable interest in fluid flow regulation [6–8]. Furthermore, fluid flow in lymphatic structures suggests direct connections between brain ISF, fluid channels, vascular structures and cervical and spinal lymph nodes. However, it is difficult to demonstrate CSF convection in the densely packed, incompressible cerebral grey matter [5, 9–12].

An often-overlooked source of convection is metabolic water, which is produced by the metabolic pathways that involve glucose, lactate, other supplemental or alternative fuels, and ATP. In humans, the brain consumes approximately 20% of our metabolic energy, despite comprising only 2% of our body mass. This renders it one of the most energetically costly organs in the body. In contrast to the majority of other tissues, which demonstrate considerable flexibility in the type of food that can be extracted and consumed from the blood, the normal brain is almost exclusively restricted to glucose as a substrate for its energy metabolism [13]. In this study, we sought to quantify the metabolic water produced by brain glucose catabolism, which may contribute to brain fluid flow. Our findings suggest that intrinsic metabolic water production plays a key role in both the ISF-CSF flow and lymphatic flow. The paper describes the cellular and subcellular sites of metabolic water production and compares the calculated amounts of metabolic water produced by neurons and astrocytes during different activity states (rest, stimulation, deep sleep).

Glucose oxidation, metabolic water, and mitochondria

Theoretical stoichiometry of glucose oxidation

It is widely recognized that oxidation of glucose (Glc) in brain and other organs produces CO_2 and H_2O, with the following stoichiometry [14–19]:

$$\text{glucose } (C_6H_{12}O_6) + 6\,O_2 \rightarrow 6\,H_2O + 6\,CO_2. \quad (1)$$

This water is denoted as 'metabolic water', as opposed to water derived from ingested fluids or substrates that enter blood and can cross the blood–brain barrier (BBB) and CSF that is produced by the choroid plexus. Despite continuous water production from metabolism of glucose in brain cells, the fates and functions of metabolic water are poorly understood. Previous estimates of brain metabolic water production based on Eq. (1), i.e., 6 H_2O/glucose [14–16, 18, 19], are too low, and higher values are obtained with the stoichiometry of biochemical reactions of glucose oxidation as described below (see Sect. "Metabolic water production during glucose metabolism in resting, awake, non-stimulated subjects").

Mitochondria produce metabolic water

Most metabolic water is generated in mitochondria by cytochrome c oxidase during the electron transport process and by ATP synthase during oxidative phosphorylation, and the main sinks for metabolic water are cytosolic hydrolytic reactions, extracellular fluid, and blood. Water fluxes from mitochondria to the cytosol are substantial and some of this water must ultimately leave the cell and the brain. While synaptic activity, membrane potentials, ion pumping, and other ATP-requiring processes are mainly supported by oxidative metabolism there is considerable heterogeneity of energy demands among cell types and subcellular structures [20, 21]. For example, mitochondria are heterogeneously distributed among brain regions [22], only about half of the presynaptic structures contain mitochondria [23, 24], and the fine peripheral astrocytic processes that surround synaptic elements contain many small mitochondria [25].

Metabolic water production rate approximates perivascular-lymphatic drainage rate

Based on Equation (Eq. (1)), a rough estimate of metabolic water production in rat cerebral cortex can be calculated from a rate of glucose utilization (CMR_{glc}) of ~ 1 µmol/g/min [26] and nearly all (90–95%) of the glucose being oxidized in the resting awake unstimulated state [13]: 1 Glc × 6 H_2O/Glc = 6 µmol H_2O/g/min × 18 µg H_2O/µmol × 10^{-3} µL/µg = 0.11 µL/g/min, which approximates the rates of ISF drainage to the lymphatic system, i.e., ~ 0.1–0.3 µL/g/min in regions of rat and rabbit brain [27, 28]. The similarity of these rates raises the question whether metabolic water may contribute to and help drive the brain's fluid flow to lymph nodes and support other water fluxes generated by local osmotic changes during cellular activity.

Regional rates of metabolic water production vary with local CMR_{glc} and are lower than CSF formation

Glucose utilization rates vary widely among brain structures and among species, with regional CMR_{glc} in human and primate brain being about half those in the rat [29],

and metabolic water production would be correspondingly lower than in the rat (see below, Sect. "Calculated rates of metabolic water production at the cellular level", Table 1, Fig. 5). For example, CMR_{glc} in cerebral cortex of resting awake humans is 0.37 μmol/g/min (Table 1), and metabolic water production based on 6 H_2O/Glc would be ~ 0.04 μL/g/min. However, as discussed below, metabolic water produced by enzymatic reactions of glucose oxidation amounts to 38 molecules of water per glucose, approximately 10 of which may be secreted, so the above values are minimal rates and adjusted values are higher: for the rat, 0.11 x (10/6) = 0.18 μL/g/min and for the

Table 1 Calculated rates of cellular metabolic water production during rest and activation

Species, brain region, pathway, cell type, and reference	CMR_{glc} (μmol/g/min)		Total H_2O/Glc[a] (μL/g/min)		Secreted H_2O/Glc[b] (μL/g/min)		Total H_2O/Glc (ml/brain/day)	Secreted H_2O/Glc (ml/brain/day)
Rat	**Rest[c]**	**Stim.[d]**	**Rest**	**Stim**	**Rest**	**Stim**	**Rest**	**Rest**
Whole brain								
CBF x AV_{glc} [146, 147]	0.67		0.46		0.12		1.31	0.35
Weighted average [^{14}C]DG [148]	0.69		0.47		0.12		1.35	0.36
[^{13}C]Glc MRS [e] [142]	0.91		0.62		0.16		1.78	0.47
$CMR_{glc\text{-}ox\text{-}a}$	0.33		0.22		0.06		0.65	0.17
$CMR_{glc\text{-}ox\text{-}n}$	0.57		0.39		0.10		1.12	0.30
Cerebral cortex, [6-^{14}C]Glc [f] [111]	0.74	0.93	0.50		0.13		0.73	0.19
$CMR_{glc\text{-}ox\text{-}a}$	0.14	0	0.09		0.02	0	0.14	0.04
$CMR_{glc\text{-}ox\text{-}n}$	0.60	0.47	0.41	0.32	0.11	0.07	0.59	0.15
$CMR_{glc\text{-}nonox\text{-}n}$	0	0.47		0.02		0		
$CMR_{glycogen\text{-}nonox}$	0	0.54	0	0.02	0	0		
Human								
Whole brain								
CBF x AV_{glc} [32]	0.23		0.16		0.04		315	84
[^{18}F]FDG PET [149]	0.23		0.16		0.04		315	84
[^{18}F]FDG PET-gray matter [150]	0.28		0.19		0.05		384	102
Cerebral cortex [^{13}C]Glc MRS [g] [46]	0.37	0.49	0.25		0.07		380	101
$CMR_{glc\text{-}ox\text{-}a}$	0.07	0	0.05		0.01	0	72	19
$CMR_{glc\text{-}nonox\text{-}a}$	0							
$CMR_{glc\text{-}ox\text{-}n}$	0.30	0.25	0.20	0.17	0.06	0.03	308	82
$CMR_{glc\text{-}nonox\text{-}n}$	0	0.25		0.01	0	0		

CMR_{glc}, rate of glucose utilization; where subscripts denote the pathway and cell type of Glc metabolism: $_{ox}$, oxidized; $_{nonox}$, nonoxidized, -a astrocyte, -n, neuron; Rest denotes the resting (physically inactive), awake, non-stimulated subject; Stim., sensory stimulation to activate metabolism in cortical regions; CBF, cerebral blood flow rate; AV_{glc}, arteriovenous difference for glucose; DG, 2-deoxyglucose; Glc, glucose; MRS, magnetic resonance spectroscopy; FDG, fluorodeoxyglucose; PET, positron emission tomography

[a] Rates of total water production were calculated as the product of metabolic rate in that pathway and the water formed per glucose, then converted to volume: (μmol Glc/g/min)*(X μmol H_2O produced per pathway/Glc)*(18 μg H_2O/μmol H_2O)*(10^{-3} μL/μg H_2O), where X = 38 for oxidation and 2 for glycolysis during rest and activation for both neurons and astrocytes. Total and secreted water per day were calculated based on rat whole brain and cerebral cortex weights of 2 g and 1 g, respectively. The relative size of human cerebral cortex is about 75% of the entire brain mass or volume [151], i.e., 1050 g for a 1400 g brain

[b] Rates of secreted water production were calculated as: (μmol Glc/g/min)*(X μmol H_2O secreted per pathway/Glc)*(18 μg H_2O/μmol H_2O)*(10^{-3} μL/μg H_2O), where X = 10 for oxidation during rest, 8 for oxidation during stimulation, and 0 for glycolysis during stimulation

[c] In resting, awake, non-stimulated subjects ~ 90–95% of the glucose is oxidized; for simplicity, nonoxidative metabolism is assigned to zero and $CMR_{glc} = CMR_{glc\text{-}ox}$

[d] Sensory stimulation and physical activity increase brain metabolism with a disproportionate rise in non-oxidative metabolism in rats [110, 146] and humans [32, 33]. Based on the glucose sparing by glycogenolysis model [46], glycogen is the sole fuel for astrocytes during stimulation and $CMR_{glc\text{-}a}$ is zero. Accordingly, measured CMR_{glc} is assigned to neurons, with about half oxidized and half nonoxidized

[e] The calculated resting value for whole brain CMR_{glc} is ~ 30% higher than other reports, perhaps influenced by postmortem ischemic changes in metabolite levels (due to decapitation followed by freezing the heads in liquid nitrogen) that may affect calculated pathway rates (Also see Fig. 5 legend)

[f] The cellular basis of CMR_{glc} at rest was not measured in this study and the proportion oxidized by astrocytes (18%) and neurons (82%) was based on the mean $CMR_{glc\text{-}ox\text{-}n}$ (0.30) for human brain tabulated in the Supplemental Information (SI) Table SI-9 of reference [46] and the mean $CMR_{glc\text{-}ox\text{-}a}$ (0.07) reported in the references cited in Table SI-9. During activation measured CMR_{glc} was assigned to neurons and glycogenolysis to astrocytes. Our previous studies [40, 43] demonstrated upregulation of nonoxidative metabolism that during activation to produce labeled and unlabeled lactate that is rapidly released from the brain. Rapid lactate release causes underestimation of CMR_{glc} and the non-oxidized fraction in [^{14}C]DG assays in rats and in [^{13}C]glucose MRS studies in rats and humans (see text)

[g] The glucose utilization rates in neurons and astrocytes are mean values of literature reports summarized in reference [46] in their Supplemental Information (SI) Tables SI-6, SI-7, SI-8, and SI-9. Anesthesia alters metabolism, and only values from awake subjects were included in the means

human 0.04 x (10/6) = 0.07 μL/g/min (see Sect. "Calculated rates of metabolic water production at the cellular level", below). As a reference, cerebrospinal fluid production rates range from about 0.23–0.81, 0.2–1.7, and 0.2–0.86 μL/g/min in mice, rats, and humans, respectively (these rates were converted from units of μL/min reported in Table 1 of [30] using brain weights of ~ 0.4, 2, and 1400 g for mouse, rat, and human, respectively).

The following discussion of brain metabolic water production is based on the mechanistic stoichiometry of reactions of glucose metabolism, with the goal of increasing attention to potential contributions of metabolic water to the brain's fluid dynamics.

Metabolic water production during glucose metabolism in resting, awake, non-stimulated subjects

The schematic in Fig. 1 illustrates the pathways of metabolic water production by oxidative metabolism of glucose. The Appendix Sect. "Reactions that consume and produce water during metabolism of glucose", Fig. 8, and Table 2 present the details of the reactions in the glycolytic pathway, tricarboxylic acid (TCA) (citric acid) cycle, electron transport chain, and oxidative phosphorylation that consume or produce water or ATP. Oxidation–reduction reactions involving NAD^+ and FAD are also included since they are involved in water and ATP production.

Glycolysis and TCA cycle

Conversion of 1 Glc to 2 pyruvate (Pyr) via glycolysis produces 2 H_2O via the enolase reaction (Fig. 1) and a net gain of 2 ATP by substrate-level phosphorylation reactions (Also see Appendix Sect. "Reactions that consume and produce water during metabolism of glucose", Fig. 8, Table 2). On the other hand, oxidation of 2 Pyr in the TCA cycle consumes 4 H_2O (Fig. 1), 2 each at the citrate synthase and fumarase steps, and generates 2 GTP (= 2 ATP) by substrate-level phosphorylation at the succinyl CoA synthetase step. Thus, in glycolysis and the TCA cycle there is a net consumption of 2 H_2O and net production of 4 ATP, 10 NADH + 10 H^+ and 2 $FADH_2$ per glucose oxidized (Fig. 8 and Table 2).

Redox shuttling from cytosol to mitochondria

Under resting, awake, non-stimulated conditions ~ 90–95% of the glucose is oxidized, based on the ratio of oxygen to glucose utilization (CMR_{O2}/CMR_{glc}) determined in human and rat brain to be 5.5–6, close to the theoretical maximum of 6, Eq. (1) [13]. Therefore, most of the reducing equivalents produced by glycolysis in the cytosol are transferred to the mitochondria by the malate-aspartate shuttle (MAS) where they enter the electron transport chain (Fig. 8, Table 2). A small fraction of the NADH + H^+ is used to reduce pyruvate to lactate and regenerate NAD^+. However, during activation [13, 31], mental work [32], and physical exercise [33], glycolysis is upregulated much more than the modest increase in CMR_{O2} that rises up to about 20–25%, along with net production and release of lactate.

Electron transport chain (ETC) and oxidative phosphorylation

The ETC transfers electrons from NADH + H^+ and $FADH_2$ and pumps protons from the mitochondrial matrix to the intermembrane space to create an electrochemical gradient that is used to drive ATP synthesis (Fig. 1). Cytochrome c oxidase transfers the electrons to oxygen to generate water, with a yield of 12 H_2O per glucose oxidized (Figs. 1, 8, Table 2). Oxidative phosphorylation uses the proton gradient to drive the ATP synthase reaction, producing ~ 2.5 ATP from each NADH + H^+ and ~ 1.5 ATP per $FADH_2$ [34]. Assuming all glucose is oxidized, a net of 28 ATP and 28 H_2O are generated (Figs. 1, 8, Table 2).

The pentose phosphate shunt and glycogen synthesis consume water, but the rates of these pathways are low in resting, awake non-stimulated subjects and the small amounts of water are not included in the metabolic water budget (For details, see Sect. "Metabolic water during metabolism of Glc-6P via branch pathways" and Table 2).

Summary

The stoichiometry of glucose metabolism with water and ATP production by biochemical oxidation of the glucose is as follows (Table 2):

$$\begin{aligned} &\mathrm{Glc} + 32\,\mathrm{ADP} + 32\,\mathrm{Pi} + 6\,\mathrm{O_2} \\ &\rightarrow 6\,\mathrm{CO_2} + 32\,\mathrm{ATP} + 38\,\mathrm{H_2O}. \end{aligned} \quad (2)$$

Enzymatic oxidation of glucose to produce energy to satisfy the demands of cells produces a net of 38 H_2O, 32 more than the 6 H_2O anticipated by the mass balance reaction in Eq. (1). Continuous glucose oxidation generates metabolic water in the mitochondrial matrix that transits to the cytosol, with efflux to ISF.

Influence of ATP turnover on metabolic water utilization

Water consumption by hydrolytic reactions

Substrate-level phosphorylation in the glycolytic and TCA cycle pathways involves the direct transfer of a phosphoryl group to ADP or GDP from a 'high-energy' compound (e.g., 1,3-bisphosphoglycerate, phosphoenolpyruvate, succinyl CoA) without the involvement of a water molecule, contrasting water production by ATP

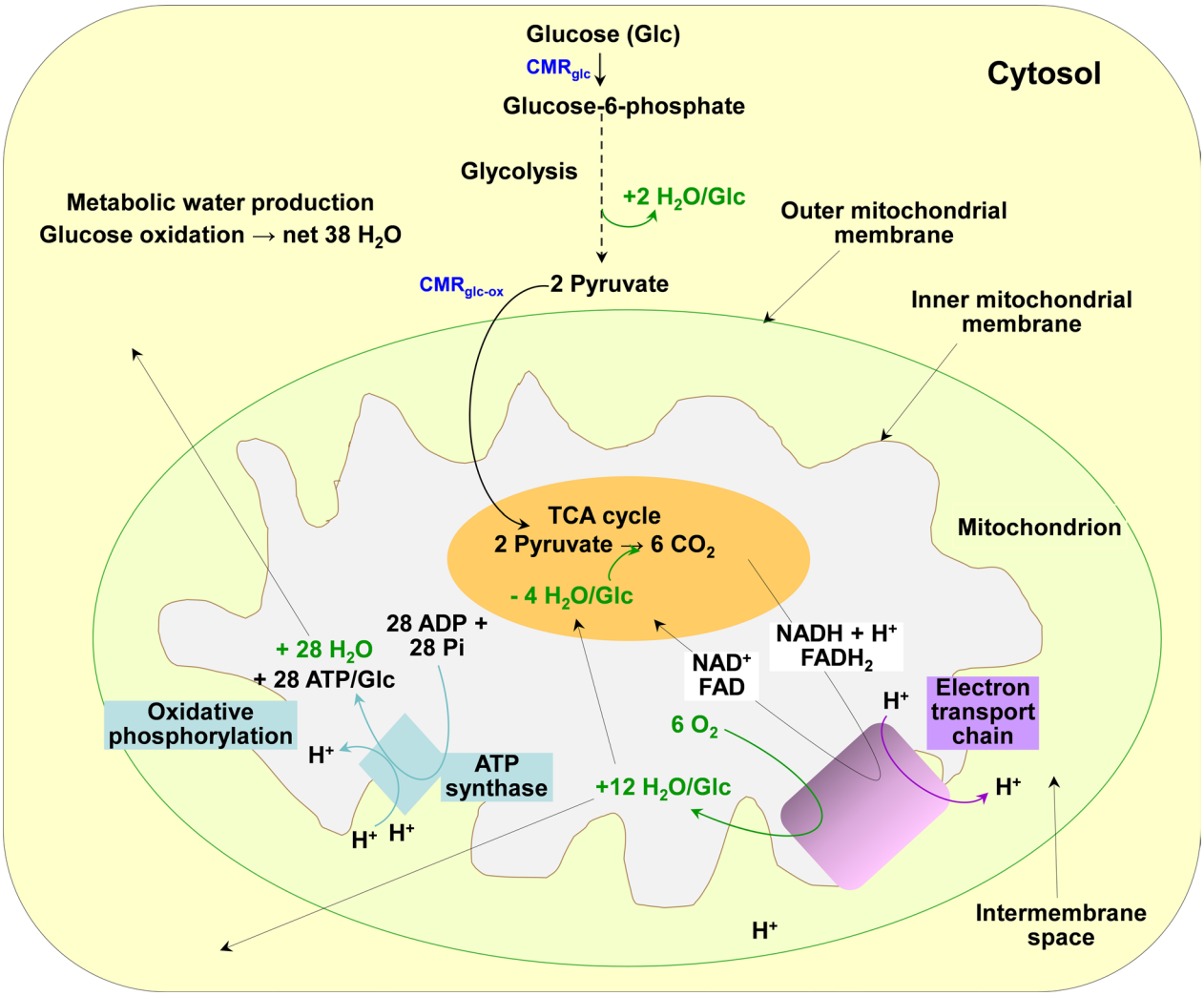

Fig. 1 Metabolic water is produced in different pathways of glucose metabolism. CMR_{glc} represents the glucose utilization rate, as determined at the hexokinase step. The $CMR_{glc\text{-}ox}$ represents the rate of glucose oxidation, which is equivalent to half of the TCA cycle rate when all glucose is oxidized. This is because the cycle rate is twice that of CMR_{glc}, with two pyruvate molecules produced per glucose molecule. The glycolytic pathway, the electron transport chain, and oxidative phosphorylation are the sources of metabolic water, which is produced and indicated by a plus sign. Conversely, the TCA cycle and cytosolic energy-dependent reactions that utilize hydrolysis consume metabolic water, indicated by a minus sign. The efflux of water across the mitochondrial membrane is significantly greater than the influx of pyruvate. Most of the water produced by the electron transport chain and oxidative phosphorylation is released to the cytosol, where it can be utilized for hydrolytic reactions or secreted into interstitial fluid. This flux is continuous, directional, and varies in accordance with the rate of glucose oxidation. For further details, please refer to Appendix Sects. "Reactions that consume and produce water during metabolism of glucose" and "Metabolic water during metabolism of Glc-6P via branch pathways", Fig. 8, and Table 2

synthase ($ADP + Pi \rightarrow ATP + H_2O$). The hexokinase, phosphofructokinase, adenylate kinase ($AMP + ATP \leftrightarrow 2\ ADP$), protein kinase A, and other ATP-dependent enzymes also involve direct transfer of the phosphoryl group from ATP in a nucleophilic reaction, without involvement of a water molecule in the mechanism [17]. This contrasts with ATP hydrolysis that involves water consumption ($ATP + H_2O \rightarrow ADP + Pi$) by the major ion pumps in brain, e.g., Na^+, K^+-ATPase, Ca^{2+}-ATPase, H^+-ATPase, and other enzymes [35]. For clarity, cation pumps illustrated in Figs. 2, 3 and 4 are placed at the plasma membrane where Na^+, K^+-ATPase is prominent, but pumps are also on vesicles (H^+-ATPase) and endoplasmic reticulum (Ca^{2+}-ATPase).

ATP concentration versus ATP production rate

The brain ATP concentration is ~ 2.3–3.1 μmol/g [16], indicating that its turnover (i.e., synthesis-utilization)

Table 2 Reactions of glucose metabolism that produce or consume water, NADH, $FADH_2$, or ATP/GTP

Enzyme	Reaction	H_2O/reaction	H_2O/Glc	ATP or GTP/Glc	NADH or $FADH_2$/Glc
A. **Glycolysis**	**Glc → 2 Pyr**				
Hexokinase	Glc + ATP → Glc-6P + ADP			−1	
Phosphoglucose isomerase	Glc-6P ↔ Fru-6P				
Phosphofructokinase	Fru-6P + ATP → Fru-1,6P_2 + ADP			−1	
Aldolase	Fru-1,6P_2 ↔ Gal-3P + DHAP				
Triosephosphate isomerase	Gal-3P ↔ DHAP				
Glyceraldehyde 3-P dehydrogenase[a]	Gal-3P + **Pi**[a] + NAD^+ ↔ 1,3-bisphosphoglycerate + NADH + H^+	0[a]	0[a]		+2
Phosphoglycerate kinase[a]	1,3-bisphosphoglycerate + ADP ↔ 3P-glycerate + ATP			+2	
Phosphoglycerate mutase	3P-glycerate ↔ 2P-glycerate				
Enolase	2P-glycerate ↔ PEP + **H_2O**	+1	+2		
Pyruvate kinase[a]	PEP + ADP → Pyr + ATP			+2	
Malate-Aspartate shuttle[b]	(2NADH + $2H^+$)cytosol → (2NADH + $2H^+$)mitochondria to enter electron transport chain				
	Net from 1 Glc → 2 Pyr[b] (1 Pyr + NADH + H^+ → lactate + NAD^+)[b]	**+1** (+1)	**+2**[a] (+2)	**+2** (+2)	**+2** (0)[b]
B. **Citric acid (TCA) cycle**	**Pyr → 3 CO_2**				
Pyruvate dehydrogenase	Pyr + CoASH + NAD^+ → Acetyl CoA + **CO_2** + NADH + H^+				+2
Citrate synthase	Acetyl CoA + OAA + **H_2O** ↔ citrate + CoASH	−1	−2		
Aconitase	Citrate ↔ isocitrate				
Isocitrate dehydrogenase	Isocitrate + NAD^+ → αKG + **CO_2** + NADH + H^+				+2
αKG dehydrogenase	αKG + NAD^+ + CoASH → Succinyl CoA + **CO_2** + NADH + H^+				+2
Succinyl CoA synthetase[a]	Succinyl CoA + **Pi**[a] + GDP → Succinate + GTP + CoASH	0[a]	0[a]	+2 GTP	
Succinate dehydrogenase	Succinate + FAD ↔ fumarate + $FADH_2$				+2$FADH_2$
Fumarase	Fumarate + **H_2O** ↔ L-malate	−1	−2		
NAD-L-malate dehydrogenase	L-Malate + NAD^+ ↔ OAA + NADH + H^+				+2
	Net from 1 Glc via glycolysis + TCA cycle	**−1**	**−2**[a]	**+4**	**10 NADH + 2 $FADH_2$**
C. **Electron transport** Water produced from transfer of electrons from NADH and $FADH_2$ to O_2 via Complexes I to IV along with pumping H^+ from the matrix to IMS (17)	NADH + H^+ → 2 e^- + NAD^+ (Complex I) ~10 H^+_{matrix} → 10 H^+_{IMS} per 2e^- through Complex I to IV 10 NADH + 10 H^+ per Glc				
	$FADH_2$ → 2e^- + FAD (Complex II) ~6 H^+_{matrix} → 6 H^+_{IMS} per 2e^- through Complex II to IV 2 $FADH_2$ per Glc				
	2 e^- + ½ O_2 + 2 H^+ → H_2O (Complex IV) ~2 H^+_{matrix} → 2 H^+_{IMS} per 2 e^- though Complex IV				
	Net: ~10×10 H^+_{matrix} + ~6×2 H^+_{matrix} → 112 H^+_{IMS}				
	Net: 6 O_2 + 24 H^+ → 12 H_2O		+12		

Table 2 (continued)

Enzyme	Reaction	H_2O/reaction	H_2O/Glc	ATP or GTP/Glc	NADH or $FADH_2$/Glc
D. **ATP synthase** Dissipation of the IMS-matrix H^+ gradient formed during electron transport is used by proton-translocating ATP synthase (Complex V) to drive synthesis of ATP + H_2O (17). H^+/Pi transport into the mitochondria consumes 1 H^+ per Pi and, with proton leakage, reduces the stoichiometry of H^+ consumed per ATP synthesized (17)	30 H^+_{IMS} + 30 Pi_{IMS} → 30 H^+_{matrix} + 30 Pi_{matrix} (symport)				
	nH^+_{IMS} + ADP + Pi → ATP + H_2O + nH^+_{matrix} (ATP synthase)				
	n ≈ P/O ratio [34]				
	~ 2.5 ATP/NADH × 10 NADH/Glc = 25 ATP + 25 H_2O		+ 25	+ 25	
	~ 1.5 ATP/$FADH_2$ × 2 $FADH_2$/Glc = 3 ATP + 3 H_2O		+ 3	+ 3	
	Net: 28 ATP + 28 H_2O				
	Total of ~ 112 H^+ translocated minus 30 H^+ for Pi transport into matrix for ATP and GTP synthesis minus nH^+ for proton leaks = < ~ 82 H^+ to generate 28 ATP by ATP synthase. 82/28 = ~ 2.9 H^+ pumped /ATP by ignoring proton leak and consumption of H^+ for other processes that together reduce the P/O ratios to ~ 2.5 and ~ 1.5. For details, see discussions in references [17, 34]				
E. **Summary: Net water from metabolism of 1 Glc**	**Glycolysis + TCA cycle + electron transport + oxidative phosphorylation via ATP synthase:** 1 Glc + 32 ADP + 32 Pi + 6 O_2 → 6 CO_2 + 38 H_2O + 32 ATP **Glycolysis + TCA cycle + electron transport:** 1 Glc ($C_6H_{12}O_6$) + 6 O_2 → 6 CO_2 + 10 H_2O **Calorimetry (mass balance):** 1 Glc ($C_6H_{12}O_6$) + 6 O_2 → 6 CO_2 + 6 H_2O		**+ 38**	**+ 32**	
F. Pentose phosphate pathway Production of NADPH for management of oxidative stress and for reductive biosynthesis and ribose-5P for nucleotide biosynthesis	**3 Glc-6P + 6 $NADP^+$ + 3 H_2O → 6 NADPH + 6 H^+ + 3 CO_2 + 2 Fru-6-P + 1 Glyceraldehyde-3P (Gal-3P)**				
Glc-6P dehydrogenase	Glc-6P + 2$NADP^+$ + **H_2O** → 2 NADPH + 2 H^+ + CO_2 + ribulose-5P (Ru-5P)	+ 1	+ 1		NADPH
Ribulose-5P isomerase	Ru-5P ↔ ribose-5P (R-5P)				
Ribulose-5P epimerase	Ru-5P ↔ Xyulose-5P (Xu-5P)				
Transketolase	R-5P + Xu-5P ↔ sedoheptulose-7-P (S-7P) + Gal-3P $C_5 + C_5$ ↔ $C_7 + C_3$ (Subscripts denote the number of carbons (C))				
Transaldolase	S7P + Gal-3P ↔ Fru-6P + erythrose-4P (E-4P) $C_7 + C_3$ ↔ $C_6 + C_4$				
Transketolase	E-4P + Xu-5P ↔ Fru-6-P + GAP → glycolytic pathway $C_5 + C4$ ↔ $C_6 + C_3$				
	Net: per 3 Glc via the PPP	**+ 1**	**+ 3**		**+ 6**

Table 2 (continued)

Enzyme	Reaction	H_2O/reaction	H_2O/Glc	ATP or GTP/Glc	NADH or $FADH_2$/Glc
G. Glycogen Glucose storage and mobilization mainly in astrocytes	**Synthesis: Glc-6P ↔ Glc-1P** **Glc-1P + $(Glycogen)_{n\ residues}$ → $(Glycogen)_{n+1}$** **Degradation: $(Glycogen)_{n\ residues}$ + Pi → $(Glycogen)_{n-1}$ + Glc-1P** **Glc-1P ↔ Glc-6P → glycolytic pathway**				
Phosphoglucomutase	Glc-6P ↔ Glc-1P				
UDP-Glc pyrophosphorylase	UTP + Glc-1P ↔ UDP-Glc + PPi (pyrophosphate)	0	0	-1	
Inorganic pyrophosphatase	PPi + **H_2O** → 2 Pi	+1	+1		
Glycogen synthase	UDP-Glc + $(Glycogen)_{n\ residues}$ → $(Glycogen)_{n+1}$ + UDP				
Glycogen phosphorylase	$(Glycogen)_n$ + Pi → $(Glycogen)_{n-1}$ + Glc-1P (1 glucosyl unit)				
Phosphoglucomutase	Glc-1P ↔ Glc-6P				
	Net for synthesis of 1 glucosyl unit from Glc-6-P	**+1**	**+1**	**-1**	
	Net for degradation of 1 glucosyl unit to Glc-6-P	**0**	**0**	**0**	
	1 Glycogen glucosyl unit → glycolytic pathway → 2 Lactate	**+1**	**+2**	**+3**	**0**
	1 Glycogen glucosyl unit → oxidative pathway → $3CO_2$		**+38**	**+33**	

Abbreviations are the same as for Fig. 8, with the following additions: Glc-1P, glucose-1-phosphate; PPi, pyrophosphate; IMS, intermembrane space between the inner and outer mitochondrial membranes. (Related to Figs. 1, 8)

The bolded text summarizes the net results for each pathway and identifies important items.

[a] Substrate-level phosphorylation involves the direct transfer of a phosphoryl group to ADP or GDP from a 'high-energy' compound (e.g., 1,3-bisphosphoglycerate, phosphoenolpyruvate, succinyl CoA) without the involvement of a water molecule, as is the case of oxidative phosphorylation and ATP synthase (ADP + Pi → ATP + H_2O). Note that hexokinase, phosphofructokinase, adenylate kinase, protein kinase A, and other enzymes also involve direct transfer of the phosphoryl group from ATP, without involvement of a water molecule in the mechanism, contrasting ATP hydrolysis (ATP + H_2O → ADP + Pi) (See main text for more details)

[b] Under resting, awake, non-stimulated conditions ~ 90–95% of the glucose is oxidized, and the reducing equivalents produced by glycolysis in the cytosol are transferred to the mitochondria by the malate-aspartate shuttle where they enter the electron transport chain. A small fraction of the Pyr is converted to lactate by lactate dehydrogenase thereby regenerating NAD^+

must be high based on production of 32 µmol ATP/g/min or 0.5 µmol ATP/g/sec when CMR_{glc} is 1 µmol/g/min. This ATP synthesis rate requires the equivalent quantities of precursor molecules, 32 µmol ADP + 32 µmol Pi/g/min that would be produced by ATP utilization (Figs. 1, 2, 8). Indeed, measured rates of Pi → ATP in human and animal brain are in good agreement with calculated values based on Eq. (2) [36, 37]. This means that ATP turns over rapidly and when the ATP concentration is constant, synthesis of ATP matches its utilization rate. Most of the metabolic water produced by oxidative phosphorylation and ATP synthase (or its equivalent derived from blood) would be consumed by ATP hydrolysis (1:1 stoichiometry for H_2O:ATP) and other processes (Fig. 2).

If the ATP synthase reaction is considered separately from glycolysis, TCA cycle, and electron transport (these processes can be experimentally distinguished, e.g., by dissipating the proton gradient to uncouple electron transport from oxidative phosphorylation), then the net water produced by glucose metabolism via glycolysis, TCA cycle, and electron transport is (38–28) = 10 H_2O/glucose (Figs. 2, 8, Table 2):

$$\mathrm{Glc} + 6\,\mathrm{O_2} \rightarrow 6\,\mathrm{CO_2} + 10\,\mathrm{H_2O}. \quad (3)$$

In other words, if ATP turnover accounts for most or all the water produced by oxidative phosphorylation, then there can be a net efflux from the cytosol and brain of 10 H_2O per glucose oxidized (Fig. 2). This amount of metabolic water exceeds the 6 H_2O predicted by the mass balance reaction Eq. (1) (for details, see Sect. "Discordant metabolic water amounts: calorimetric versus enzymatic glucose oxidation").

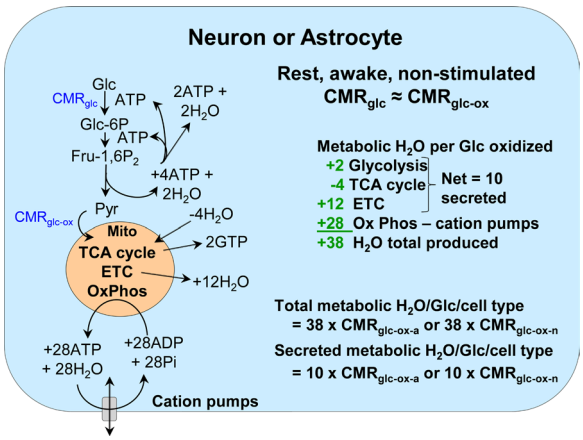

Fig. 2 Metabolic water production and utilization in the resting, awake, non-stimulated subject. The glycolysis pathway consumes two ATP and produces four ATP per glucose (Glc) metabolized, resulting in a net gain of two ATP along with the formation of two H_2O by the enolase reaction. The TCA cycle in mitochondria (Mito) consumes (denoted by a negative sign) four water molecules per glucose oxidized, with the production of 12 and 28 water molecules, respectively, occurring in the electron transport chain (ETC) and oxidative phosphorylation (OxPhos) steps. Cation pumps hydrolyze ATP and consume H_2O. Given the high turnover of ATP, it is assumed that the water produced by OxPhos is consumed by cation pumping. In the absence of any other stimuli, biosynthetic and other "housekeeping" reactions consume ATP. The net amount of H_2O produced by glycolysis, the tricarboxylic acid (TCA) cycle, and the electron transport chain (ETC) is assumed to be available for secretion. The total metabolic water production is 38 H_2O/glucose of which 10 is available for secretion. The respective rates of metabolic water production are obtained by multiplying the measured rate of glucose oxidation (CMR_{glc-ox}) in the astrocyte (-a) or neuron (-n) (see Table 1). The following abbreviations are used: Glc-6P represents glucose-6-phosphate, while Fru-1,6P_2 denotes fructose-1,6-bisphosphate. For further details, please refer to Sects. "Reactions that consume and produce water during metabolism of glucose" and "Metabolic water during metabolism of Glc-6P via branch pathways", Fig. 8, and Table 2

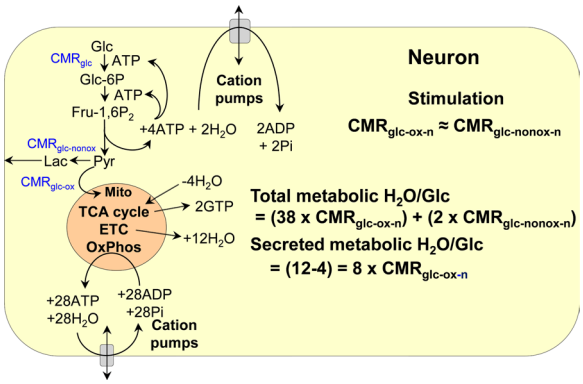

Fig. 3 Metabolic water production in activated neurons. Given the rapid fluctuations in neuronal activity, it is not feasible to rely on a timely increase in oxygen delivery with each sudden surge. Therefore, the energetic needs are met by rapid rises in glycolysis. Glycolysis of 1 glucose (Glc) molecule produces 4 ATP, 2 of which replace the ATP used to produce glucose-6P (Glc-6P) and fructose-1,6-bisphosphate (Fru-1,6P_2). The remaining 2 ATP and the 2 glycolytic H_2O are assigned to cation pumping indicated in the upper part of the figure, along with ATP/H_2O from oxidative phosphorylation (OxPhos) in mitochondria (Mito) shown in the lower part of the figure. The net 8 H_2O from the electron transport chain (ETC) and TCA cycle can be secreted. About half of the pyruvate is converted to lactate and released from the cell ($CMR_{glc-nonox}$), and the other half is oxidized (CMR_{glc-ox}). Rates of water production and secretion are calculated as the product of the molecules of H_2O per pathway times the respective metabolic rate as shown in the right part of the figure (also see Table 1)

Summary

ATP turnover is fast and is required to provide the substrates (ADP and Pi) for mitochondrial ATP synthase. ATP hydrolysis during cation pumping consumes water in a 1:1 stoichiometry, accounting for the water produced by oxidative phosphorylation. The remaining net water/glucose derived from glycolysis, TCA cycle, and ETC are

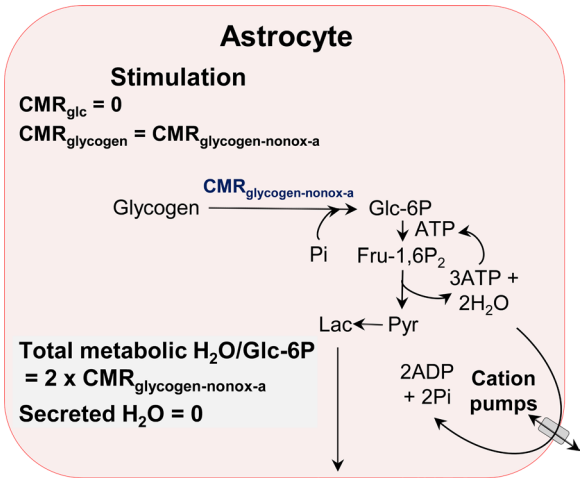

Fig. 4 Metabolic water production in activated astrocytes. Rapid fluctuations in brain activity trigger an increase in astrocyte metabolism associated with glutamate uptake, conversion of glutamate to glutamine, and the associated cation pumping. Astrocytic energy requirements are met by glycogenolysis, a pathway that can rapidly replenish ATP [46]. Glycolytic metabolism of 1 glucose-6-phosphate (Glc-6P) molecule produces 3 ATP, 1 of which replaces that used to produce fructose-1,6-bisphosphate (Fru-1,6P2). The other 2 ATP plus 2 glycolytic H_2O are assigned to cation pumping; no metabolic water is available for secretion. Metabolic water production is twice the rate of glycogenolysis. The pyruvate (Pyr) generated from glycogen is converted to lactate (Lac) that is released from the cell

available for secretion, with different amounts from stimulated neurons and astrocytes.

Disproportionate upregulation of nonoxidative versus oxidative metabolism during activation

During increases in brain activity overall metabolism shifts from glucose oxidation in the awake non-stimulated state ($CMR_{glc} \approx CMR_{glc\text{-}ox}$) to include increased nonoxidative metabolism of glucose in neurons and of glycogen in astrocytes ($CMR_{glc\text{-}nonox} > CMR_{glc\text{-}ox}$) (Sect. "Evidence for disproportionate rise in nonoxidative metabolism during activation"). This change differentially alters metabolic water production in neurons versus astrocytes as described below.

Local metabolic assays during activation

Brain activation involves any situation (e.g., sensory stimulation, mental work, physical activity, etc.) that increases neuronal signaling and the associated energy requirements. Based on data from activation studies in humans and animals, CMR_{glc} increases more than CMR_{O2} and most of the rise in CMR_{glc} rate involves nonoxidative metabolism of blood-borne glucose in neurons with lactate release (see Sects. "Activity-dependent metabolic shift modulates metabolic water production", "Calculated rates of metabolic water production at the cellular level", "Evidence for disproportionate rise in nonoxidative metabolism during activation"). Glycogen is also consumed non-oxidatively in astrocytes, but this rate is not measured by routine CMR_{glc} assays (e.g., using [^{14}C]deoxyglucose, [^{14}C- or ^{13}C]-glucose, [^{18}F]fluorodeoxyglucose-positron emission tomography (FDG-PET), or magnetic resonance spectroscopy); glycogen must be measured separately. Glucose utilization rates during activation calculated from metabolic assays using [^{14}C or ^{13}C]glucose are too low due to incomplete product trapping in the activated tissue [38, 39] (see Sect. "Parallel assays with [14C]deoxyglucose (DG) and [1- or 6-14C] glucose"). Of glucose metabolites, lactate is the most diffusible and it quickly moves from activated cells to blood [40] and the perivascular-lymphatic drainage system [41]. Intracellular lactate in astrocytes is readily shuttled among other gap junction-astrocytes [42], so it can be quickly dispersed from activated cells via the syncytial network and released to ISF. After microinfusion of [1-^{14}C]glucose or D-[^{14}C]lactate into the inferior colliculus of the awake rat, L- or D-[^{14}C]lactate, along with [^{14}C] glucose and other labeled compounds, were recovered in the meningeal membranes, consistent with perivascular efflux [41]. The amount of [^{14}C]glucose-derived lactate released to blood during spreading depression accounted for about half the magnitude of underestimation of calculated CMR_{glc}, and the other half of the underestimation was attributed to lactate efflux via perivascular-lymphatic drainage [40, 41, 43].

Glucose sparing by glycogenolysis (GSG) model

The above experimental evidence strongly supports the model describing glucose sparing by glycogenolysis [44–46] in which (i) glycogenolysis supports astrocytic energetics during the early phase of activation (i.e., $CMR_{glc\text{-}astrocyte} = 0$), thereby sparing blood-borne glucose for neurons until endothelial glucose GLUT1 transporters are mobilized from intracellular stores to the plasma membrane [47, 48] and GLUT4 transporters are inserted into neuronal plasma membranes from internal stores in rapid response to action potential firing [49, 50], and (ii) the incremental increase in neuronal glucose oxidation equals that of neuronal nonoxidative metabolism of glucose. Major predictions of the GSG model are excellent fits to experimental data [46]. This is important because neuronal and astrocytic release of lactate osmoles to ISF during activation may enhance metabolic water secretion.

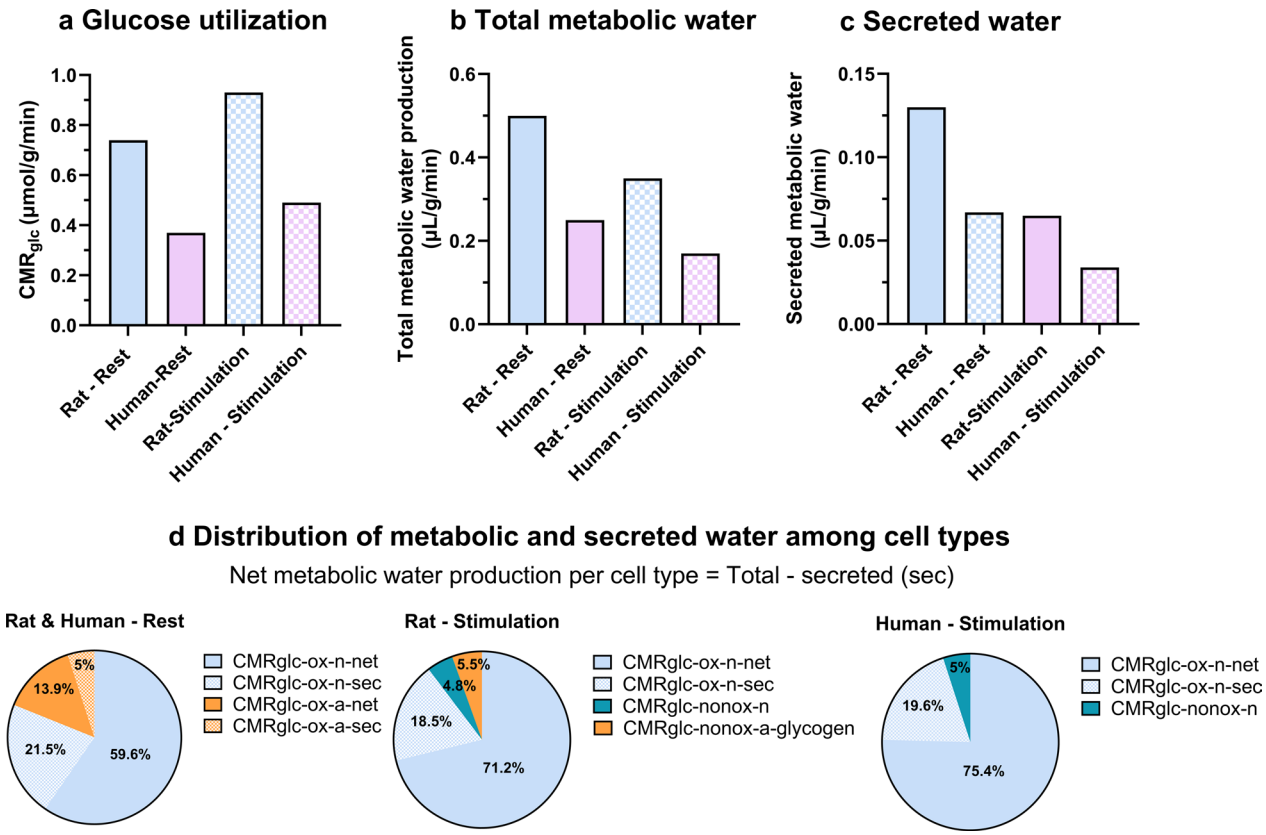

Fig. 5 Metabolic water production and secretion from glucose utilization in rat and human brain during rest and activation. Data are from Table 1. **a**. Cerebral cortical CMR_{glc} at rest is higher in rats than in humans, and in both species CMR_{glc} increases during activation. **b**. Total metabolic water generated by glucose metabolism is lower during rises in activity than during rest due to lower oxidation rates (Table 1) and higher activity of cation pumps that use water for hydrolysis of ATP. **c**. As the increase in CMR_{glc} is mainly due to glycolysis, the amount of water secreted from glucose utilization decreases during activation. **d**. Metabolic water production during rest and activation in rat and human brains for neurons and astrocytes. For both cell types the main amount of metabolic water is produced in mitochondria. The amount of secreted water is reduced by about half during stimulation because less glucose is oxidized compared with rest and more water is consumed by ATP hydrolysis during cation pumping (Table 1, Figs. 3, 4). The percentage distributions of total and secreted metabolic water are presented as the same in rat and human brain during rest (Fig. 5d), because the rat values are based on resting human data due to a limited number of MRS studies in the awake rat. Of the reports tabulated in reference [46] in its Supplemental Information (SI) Tables SI-4 and SI-5, nine of 10 MRS studies used anesthesia that alters metabolism. The whole brain CMR_{glc} (0.91 µmol/g/min, Table 1) in the single awake rat study [142] was ~ 30% higher than that determined by arteriovenous difference or weighted average of brain regions in [^{14}C]deoxyglucose assays (mean, 0.68 µmol/g/min, Table 1). In reference [142] the whole brain CMR_{glc} and the calculated cellular proportions (36% astrocyte, 63% neuron) of glucose oxidation rates are questioned because the rats were decapitated and heads frozen in liquid nitrogen, thereby causing postmortem ischemia that disrupts metabolism [143] (also see Table 1 footnotes). For this reason the astrocyte-neuron partitioning obtained in resting human brain (mean of 19% astrocyte, 81% neuron in 7 studies; Tables SI-6, 7, 9 in reference [46]) was used for calculations and figures in the resting state (Table 1, Fig. 5). Although the percent distributions in resting rat and human brain are the same, the absolute values differ (Table 1)

Summary

Activity-dependent shifts in fluxes of glucose, glycogen, and oxygen metabolism disproportionately increase nonoxidative metabolism of glucose and glycogen compared with oxidative metabolism and differentially impact metabolic water production and consumption in neurons versus astrocytes. Neurons preserve glucose oxidation and its associated metabolic water production while also increasing nonoxidative glycolytic metabolism. In contrast, astrocytes rely on glycolytic metabolism of glycogen. The 1:1 H_2O:ATP stoichiometry of elevated glycolytic metabolism of glucose and glycogen during activation (Table 2) provides both ATP + H_2O for the increased demands of cation pumps ($ATP + H_2O \rightarrow ADP + Pi$) in both cell types. Coupling glycolysis with ATP formation and hydrolysis reduces the amount of metabolic water available for secretion (Figs. 3, 4 and 5).

Activity-dependent metabolic shift modulates metabolic water production

Resting neurons and astrocytes

At steady state in resting, awake, non-stimulated subjects, glucose is continuously consumed and oxidized, water is always produced and released, rapid ATP turnover maintains a constant ATP concentration, and the rate of glucose utilization is the same as that of glucose oxidation: $CMR_{glc} \approx CMR_{glc\text{-}ox}$ (Fig. 2). This means that of the 32 total ATP produced per glucose oxidized, 4 are generated by substrate-level phosphorylation (GTP = ATP) without involvement of water, and 28 ATP are synthesized along with 28 water molecules by ATP synthase (Figs. 3, 8, Table 2). As noted above, the major cation pumps consume 1 H_2O per ATP hydrolyzed [35] and Na^+, K^+-ATPase accounts for ~ 50–65% of the brain's energy demand [13], with additional ATP and H_2O consumed by the Ca^{2+}-ATPase and H^+-ATPase activities [35]. This means that most of the ATP is hydrolyzed during cation pumping. Thus, 28 of the 38 water generated by glucose oxidation are involved in ATP turnover (Fig. 2), with a net of 10 water molecules can be released. This increases the theoretical rate of metabolic water efflux calculated above from Eq. (1) by a factor of 10/6 per glucose or 1.7-fold, from ~ 0.11 to 0.18 µL/g/min in rat brain. In contrast to the water derived from mass balance equations, calculated metabolic water production and secretion rates based on measured glucose metabolic rates in neurons and astrocytes are given in Table 1 (see Sect. "Calculated rates of metabolic water production at the cellular level", below).

Increased glycolysis in activated neurons and astrocytes

A consequence of glycolytic lactate generation during brain activation is reduced ATP and water production by the oxidative pathways. One cytoplasmic NADH + 1 H^+ are consumed per lactate formed from 1 pyruvate (Fig. 8, Table 2), pyruvate is eliminated as an oxidative substrate, and metabolic water formation by electron transport and oxidative phosphorylation is reduced by 6 and 14 H_2O, respectively, per pyruvate converted to lactate (Table 2). Thus, if cation pumping is the basis for most of the increased energy demand during activation, neuronal ion pumps can obtain water required for ATP hydrolysis from metabolic water from both glycolysis and oxidation (Fig. 3), whereas astroglia derive metabolic water only from glycolytic metabolism of glycogen (Fig. 4).

Activated neurons

Based on the GSG model, total CMR_{glc} is assigned to neurons during activation, with half oxidized and half not oxidized: $CMR_{glc\text{-}ox\text{-}n} \approx CMR_{glc\text{-}nonox\text{-}n}$ (Fig. 3). Because cation pumping is enhanced when activity rises, metabolic water produced by glycolysis and oxidative phosphorylation is assigned to ATP hydrolysis during ion pumping. Calculation of metabolic water production in activated neurons has two components, 38 H_2O/glucose from oxidation plus 2/glucose from non-oxidative glycolysis, with 8 H_2O available for secretion (Fig. 3), two less than in the resting state. Production and secretion rates are calculated from the number of water molecules produced per glucose for each pathway times the respective metabolic rate (see Sect. "Calculated rates of metabolic water production at the cellular level" and Table 1).

Activated astrocytes

Based on the GSG model, nonoxidative glycogenolysis replaces metabolism of blood-borne glucose, and $CMR_{glc\text{-}a} = 0$ (Fig. 4). Glycogen supplies glucosyl units to the Glc-6P step of glycolysis, for a net ATP yield of 3, one of which replaces the ATP used to phosphorylate Fru-6P. The remaining 2 ATP and 2 H_2O from glycolysis are assigned to cation pumping. No metabolic water is available for secretion from activated astrocytes.

Summary

Mechanistic stoichiometry of glucose utilization reactions reveals that more metabolic water is produced and secreted under resting conditions than during rises in activity. During activating conditions most metabolic water and all secreted water is derived from neuronal oxidative metabolism. Astrocytes consume glycogen and produce water that is consumed by ATP hydrolysis related to cation pumping. Based on higher glucose utilization rates in neuropil compared with cell bodies during rest and electrical stimulation [51], most metabolic water would be anticipated to be produced by synaptic compartments and perisynaptic astrocytic processes compared with neuronal soma.

Calculated rates of metabolic water production at the cellular level

Assumptions

Calculated rates of metabolic water production in whole brain, neurons, and astrocytes in rats and humans during rest and sensory stimulation are compared in Table 1. Representative glucose utilization rates were obtained from the literature and used to calculate rates of total metabolic water and secreted water production using calculation factors based on the mechanistic stoichiometric amount of water produced per glucose molecule per cell type per pathway as indicated in Figs. 2, 3, 4 and 8,

and Table 2. The assumptions used for these calculations were based on steady state homeostasis of cellular water content, i.e., metabolic water production is matched by intracellular metabolic water consumption and secretion from the cell as illustrated in Figs. 2, 3 and 4. This metabolic water budget focuses on net production, utilization, and release, and does not distinguish mixing of metabolic water with equivalent amounts from other sources.

Rates of production and secretion of metabolic water in resting, awake subjects

Nearly all glucose is oxidized under resting conditions [13], and Table 1 and Fig. 5a–c reveal that calculated metabolic water production is higher in the resting, awake, non-stimulated subjects than during sensory stimulation, and glucose oxidation provides nearly all the total and secreted water (Table 1, Fig. 5d). Neurons produce most of the metabolic water due to their higher glucose oxidation rates ($CMR_{glc\text{-}ox\text{-}n}$) compared with astrocytes ($CMR_{glc\text{-}ox\text{-}a}$), with rats having higher production rates than humans and different distributions of production and secretion of metabolic water during stimulation (Table 1, Fig. 5a–d).

However, these cellular metabolic rates are calculated per gram tissue, and if the astrocyte volume fraction in rat cerebral cortex (9.6 ± 2.8% [52]) is taken into account and $CMR_{glc\text{-}ox\text{-}a}$ is adjusted for astrocytic volume fraction by multiplying by 1/volume fraction (i.e., multiply by 11.4 ± 3.9) [52], total metabolic water production in resting rat astrocytes per cellular volume would be about twice that in neurons. For example, rat cerebral cortex $CMR_{glc\text{-}ox\text{-}a}$ is 0.09 µL/g/min (Table 1) × 11.4 = 1.0 µL/g/min versus the adjusted rate for neurons, assuming a volume fraction of about 80%, $CMR_{glc\text{-}ox\text{-}n}$ = 0.41 x (1/0.8) = 0.51.

Total metabolic water produced per day in resting subjects is on the order of 1.3 mL in rat brain and 315–385 mL in human brain, whereas secreted water is about 0.4 mL and 85–100 mL in rat and human brain, respectively (Table 1).

Stimulation-induced rises in glucose and glycogen catabolism reduce production and secretion of metabolic water

In stimulated brain CMR_{glc} was assigned to neurons based on the GSG model, with $CMR_{glc\text{-}ox\text{-}n} \approx CMR_{glc\text{-}nonox\text{-}n}$, $CMR_{glc\text{-}a} = 0$, and glycogen fueling the activated astrocytes (Table 1). Only one study in awake rats determined CMR_{glc} and $CMR_{glycogen}$ in parallel, and the rate of glycogenolysis, 0.54 µmol/g/min (Table 1), exceeded nonoxidative metabolism of glucose in stimulated rat neurons, 0.47 µmol/g/min (Table 1). No data are available for glycogenolysis in stimulated human brain.

Most metabolic water is generated by glucose oxidation, which fell from 0.14 and 0.60 µmol/g/min in resting astrocytes and neurons, respectively, to 0 and 0.47 µmol/g/min during stimulation (Table 1). As a consequence, total metabolic water production fell from 0.5 to 0.36 µL/g/min, and secreted water fell from 0.13 to 0.07 µL/g/min (Table 1); similar trends occurred in stimulated human brain (Table 1). In addition, consumption of metabolic water by increased ATP hydrolysis during ion pumping reduced water secretion in both cell types, and secreted water is only from neuronal glucose oxidation (Table 1, Figs. 3, 4, 5b, c). More lactate is generated from glucose and glycogen during stimulation (2 lactate/glucosyl unit) and it is exported, releasing from the cell 2 lactate osmoles per osmole glucose or Glc-6P.

Hypothetical availability of glycogen-bound water as source of fluid secretion

Glycogen is a hydrophilic glucose polymer, and many, but not all, studies of liver and muscle glycogen have shown an association of tissue or whole-body water content with glycogen level in a proportion of ~ 3 g water bound per g glycogen (see discussions and references cited in [53–55]). The amount of tissue water or intracellular water increases with higher glycogen concentration and falls when glycogen is consumed, but the amount of water bound to glycogen compared to 'free' water in the tissue or cells remains to be established. Similar studies have not been carried out in brain, but if bound water:glycogen is also 3:1 in brain, the amount of bound water to glycogen would be 30 µmol H_2O/µmol glucosyl unit glycogen.

Using this value and the rate of glycogenolysis in rat brain during stimulation, 0.54 µmol/g/min (Table 1), the hypothetical rate of release of bound water from glycogen would be 0.29 µL/g/min. This would increase the calculated rate of water secretion during stimulation from 0.07 (Table 1) to 0.36 µL/g/min, 2.8-fold higher than that under resting conditions, i.e., 0.13 µL/g/min (Table 1). Water bound to glycogen is not metabolic water in a strict sense, but if released because of glycogenolysis and lactate release it may contribute to increasing perivascular fluid flow during activation. This suggests that astrocytes release water during rises in activity when glycogen is mobilized.

Metabolic water from other substrates and routes

Glucose is the major fuel for the brain, but lactate and ketone bodies can also be oxidized and generate metabolic water by the same reactions as glucose oxidation.

Water fluxes can also involve aquaporins and substrate transporters. For example, the aquaporins facilitate osmotically-driven water fluxes, whereas various substrate transporters can co-transport water along with the substrate in different tissues and cell types as, for example, the GLUT glucose transporters, the SGLT Na^+-linked glucose transporter, the EAAT1 glutamate transporter, the GAT1 GABA transporter, the MCT-1monocarboxylic acid transporter, the NKCCl Na^+, K^+, $2Cl^-$cotransporter, and the KCC K^+, Cl^--cotransporter (e.g., [1, 56–62]). For more details, see Sect. "Alternative substrates and routes for water fluxes associated with metabolism".

Summary and perspective

During rest and activation, most of the metabolic water is generated by neuronal glucose oxidation in the mitochondrial matrix from which it moves to cytosol where it can be consumed by hydrolytic reactions or secreted to interstitial fluid. Much smaller amounts of metabolic water are produced by glycolysis in neurons and astrocytes; it can contribute to secretion during rest, but not during activation when it is assigned to ATP hydrolysis to support increased cation pumping. The rates of nonoxidative metabolism of glucose during activation are greatly underestimated in assays using labeled glucose that rely on quantitative trapping of all labeled metabolites due to rapid efflux of labeled lactate from the brain. Anticipated release of bound water secondary to astrocytic glycogenolysis during activation can contribute to increased water secretion that is expected to enhance perivascular lactate clearance. This is a unique, previously unrecognized role for astrocytic glycogenolysis.

The reduced amount of total and secreted water may impact the neurovascular coupling response, i.e. the rise in blood flow that accompanies rises in activity [63]. The term neurovascular coupling (NVC) is employed to describe the sequence of events by which increases in brain activity result in increases in cerebral blood flow and energy supply to the brain [64, 65]. In response to increases in brain activity, arterioles exhibit minimal dilation, whereas brain capillaries demonstrate active dilation and contribute approximately 85% of the reduction in cerebrovascular resistance [66, 67]. The neurovascular coupling response is of the greatest amplitude at the site where nerve cell activity peaks, which also exhibits the largest alterations in glucose catabolism, activity of cationic pumps, and ATP turnover [13]. The calculations presented in this paper indicate that activation of the glycolytic pathway and increases in ATP turnover reduce the continuous production of total and secreted metabolic water, which may facilitate capillary dilation. Astrocytes have a small volume fraction (~9.6% in rat cerebral cortex [52]), but glycogenolysis is predicted to release bound water during stimulation that constrains local vasodilation and drives local perivascular-lymphatic flow.

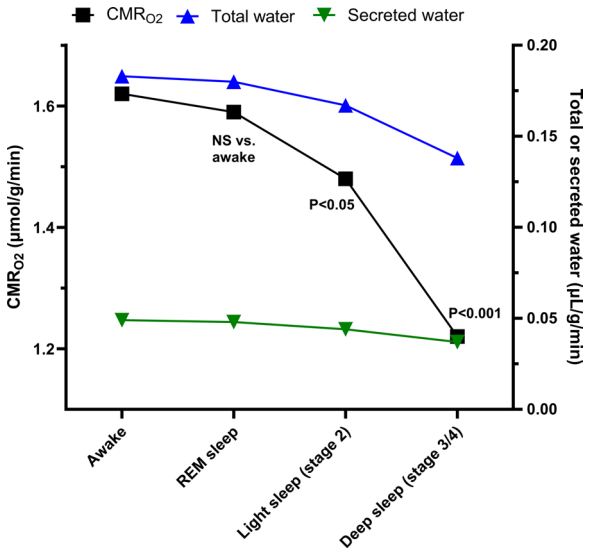

Fig. 6 Oxygen consumption during stages of sleep and calculated metabolic water production and secretion. Rates of whole-brain oxygen consumption (CMR_{O2}) in human subjects [144, 145] demonstrated no change during rapid-eye-movement (REM) sleep compared with resting, awake, non-stimulated subjects (NS, not statistically significant). However, CMR_{O2} fell significantly, by 5% and 25% during light and deep sleep, respectively, and calculated production of total water and secreted water from oxidation of glucose decreased proportionately during these sleep stages

Brain energy metabolism and calculated metabolic water production during sleep

Metabolism varies with stages of sleep

Normal human sleep is characterized by two distinct states: rapid eye movement (REM) and non-REM (NREM) sleep. The nocturnal sleep pattern of the mature human brain adheres to a predictable schedule. The onset of sleep is characterized by the transition from NREM to deeper NREM stages, which then gives way to the initial occurrence of REM sleep, typically occurring approximately 80–100 min later. Subsequently, NREM and REM sleep alternate for approximately 90 min. Stages 3 and 4 of NREM are concentrated in the initial NREM cycles, with REM sleep episodes occurring throughout the night [68]. During sleep whole brain glucose metabolism falls in parallel with systemic glucose metabolism and quantitatively accounts for a significant fraction of the reduction observed during sleep in normal humans [69]. The magnitude of CMR_{O2} during light sleep (stage II) is only moderately reduced (3–10%) in comparison to wakefulness [70]. In comparison, during deep sleep (stage III-IV),

CMR_{O2} [70] and CMR_{glc} [71, 72] are reduced by 25–44%, while during REM sleep (dreaming), global levels CMR_{O2} are approximately the same as during wakefulness [70]. The decline in brain metabolism during deep sleep is correlated with a generalized decrease in cerebral synaptic activity which is crucial to maintain brain health [73]. It is assumed that synaptic activity levels during rapid eye movement (REM) sleep, when dreaming occurs, are similar to those observed during wakefulness [74]. In accordance with this assumption, global CMR_{O2} is equivalent to that during wakefulness [70].

Calculated metabolic water production falls during deep sleep

Production and secretion of metabolic water calculated from CMR_{O2} determined during stages of sleep fell in proportion to the decrease in oxygen consumption and glucose oxidation (Fig. 6).

Summary

It is anticipated that the reduction in glucose oxidation during deep sleep (NREM) will result in a notable decrease in the secretion of metabolic water and that this may result in a reduction in the outflow of ISF to the CSF and other exit pathways. However, Xie et al. [75] reported a large, 66% increase in the extracellular volume fraction (from 14.1 to 23.4%) and increased amyloid beta clearance during slow wave sleep in mice compared with the awake state. The relationship between metabolic water production, interstitial space, and tracer clearance remain to be established. However, tracer clearance could be enhanced even when water production is reduced because blood pressure in human subjects decreases an average of 17% (described as 'nocturnal dipping') during deep sleep in most subjects [76], and lowering blood pressure by about 20% increased tracer clearance to the lymphatic system [77].

Concluding remarks and future directions

Movement of CSF, ISF, and metabolic water

The quantification of water movement between different brain cells and compartments, i.e. across the BBB, the brain-cerebral spinal fluid barrier or from the interstitial fluid compartment to the CSF or the perivascular compartments or vice versa is incompletely understood [1]. Small uncharged polar molecules such as water diffuse slowly across endothelial cell membranes and could theoretically contribute to the regulation of ISF, but the very slow diffusion rate and very low hydrostatic conductivity of the endothelium argue against diffusion or convection across capillaries as a major source of ISF. Similarly, the osmotic water permeability of the brain endothelium is very low, partly because of the complete lack of aquaporin (AQP) expression in brain endothelial cells [1], and osmotic gradients between blood plasma and CSF are small or negligible (e.g., [78–80]). Alternatively, the ISF, including metabolic water, could be assumed to diffuse between endothelial cell membranes, i.e. via the paracellular route from brain to blood. However, the volume fraction of the blood vessels is 1%, while the volume fraction of brain extracellular fluids (ECF) is 20% [81], i.e. the volume of distribution of metabolic water in the ECF is huge, and there are no mechanisms to direct metabolic water produced by neurons into the brain capillaries. In contrast, metabolic water produced by glycogenolysis in astrocytes can enter the pericapillary space via astrocyte endfeet, which are covered by AQP4 at this site [12]. The contribution of astrocytes to metabolic water under resting and activating conditions is small whereas the amount of water released by glycogen consumption during activation is greater. The transport of metabolic water to the capillaries does not guarantee transport from the brain to the blood; it can transit via the perivascular-lymphatic system (e.g., [11, 28, 82, 83]). Taken together, it is unlikely that a significant proportion of the metabolic water produced by neurons diffuses down an osmotic pressure gradient into the blood, as previously suggested may occur unless solutes mix with the metabolic water (see Sect. "Disproportionate upregulation of nonoxidative versus oxidative metabolism during activation" in [84] and Sect. "Glycolysis and TCA cycle", p. 381 in [28]).

Our hypothesis is that metabolic water, together with metabolites and waste products from neurons and astroglia, first enters the ISF surrounding the brain cells and then exits the brain via various pathways, i.e., the lymphatic vasculature or the systemic circulation via the arachnoid granulation. Notably, metabolic water is produced continuously at a slow rate and, although theoretically possible, we consider it unlikely that metabolic water produces hypotonic ECF pockets that pave the way for local osmotic transport across or between endothelial cell membranes. We suggest that metabolic water is drained along perivascular spaces and axon tracts [85] to the CSF, to lymphatic vessels along cranial or spinal nerves or the dura mater, or to the systemic circulation via arachnoid villi or fenestrated vessels after passage through the cribriform plate toward lymph nodes [6, 11, 12, 28, 82, 83, 86].

The mechanisms for the generation, flow and discharge of ISF are important and we suggest that metabolic water is a significant contributor to ISF. Bulk flow of ISF is unlikely to be of practical importance for nutrient distribution and waste removal [5], but a diffuse, continuous, global production of metabolic water may be crucial

mechanism for brain fluid flow and clearance of water-soluble waste products along perivascular spaces into the subarachnoid space, along axons to lymphatic vascular pathways, or along arachnoid granulation to the systemic circulation. Small, water-soluble metabolites are readily cleared through arachnoid granulations and fenestrated vessels, while the clearance mechanisms for larger waste products (such as amyloid-beta aggregates) is still incompletely understood [28, 87, 88]. Additional clearance routes include the glymphatic system [89–91], which appears to substantially overlap with the long-recognized perivascular-lymphatic drainage system (e.g., [11, 28, 82, 83, 92, 93] and references cited therein), and may play a role in removing both small and larger metabolic waste products from the brain. We propose that metabolic water may be a mechanism of slow, continuous bulk ISF flow, replacing or complementing CSF flow into the brain along penetrating arterioles as a mechanism and expanding the glymphatic [89] and perivascular-lymphatic [11, 28, 82] routes plus others.

In summary, capillaries play a role in fluid exchange within the brain but are not the primary route for ISF drainage. Alternative drainage pathways are critical for brain fluid dynamics and waste clearance mechanisms. Metabolic water will be critical to these mechanisms, contributing to brain homeostasis and metabolite clearance in health and disease.

Sources and drivers of fluid flow in the brain

The fluid dynamics of the brain are still incompletely understood and key questions remain unanswered [94]. Animal and human studies have identified perivascular spaces around brain arterioles and venules along which fluid, nutrients, signaling molecules, and waste products from neurons and glia can move [91], but it is unclear how and to what extent CSF bulk flow moves through brain tissue [5, 88, 89, 95].

Alternatively, one might hypothesize that metabolic water and water released by glycogenolysis may serve as sources and drivers of ISF, contributing to brain fluid formation and ultimately to lymphatic drainage along cranial and spinal nerves, or along lymphatics in the cribriform bone to retropharyngeal lymphatic vessels to the deep cervical lymph nodes [6, 7, 11, 86]. Directional flow of metabolic water from brain cells to ISF and perivascular space may also serve as a driver for clearance of lactate and other compounds [41]. Highlights of the present evaluation of the brain metabolic water budget include the following (Fig. 7):

- Glucose is the brain's energy source, and its oxidative metabolism continuously produces metabolic water, which is secreted at a similar rate as interstitial fluid is produced.
- Neuronal mitochondria produce most of the metabolic water, astrocytes less.
- Water production is greatest during rest and suppressed by rises in activity and during deep sleep.
- Ion movements induced by ongoing or evoked increases in activity trigger ion pumps that consume metabolic water through hydrolysis of ATP.
- Glycogen catabolism is anticipated to release bound water from astrocytes during activation and serve as a major fluid source for perivascular-lymphatic flow.
- The paper provides standards for calculation of metabolic water and identifies the enzymatic processes that dominate water production in neurons and astrocytes.
- These data establish metabolic water as a critical source for brain fluid production and for removal of waste products in healthy and diseased brains.

Metabolic water production varies with rates of glucose oxidation

Metabolic water is frequently mentioned in reviews of brain energy metabolism, but details of its production, the cellular and subcellular sources and sinks, and its functions in brain fluid dynamics are poorly understood. The present analysis reveals that in both the awake, non-stimulated state and during activation most metabolic water is produced by neuronal glucose oxidation. This path of glucose catabolism varies between regions, but the global consumption of glucose and oxygen is relatively constant in the resting awake state, with disproportionate upregulation of glycolysis and lactate release compared with oxidative metabolism during mental activity in the human [32] and sensory stimulation of the rat [13], whereas glucose oxidation decreases by 3–10% during light sleep and 25–44% during deep sleep [70, 72]. Hence, the global production of metabolic water is almost constant during the awake resting state, light, and REM sleep but strongly reduced during deep sleep due to the fall in oxidative metabolism. This is thought to result in a decrease in the outflow of ISF to the CSF, creating a brain-state dependent time window for CSF flow along the perivascular route from CSF to ISF [89].

In addition to variations in metabolic water production with evoked changes in rates of glucose oxidation and glucose/glycogen glycolysis in normal subjects, other factors can influence clearance of substances from brain. For example, the routes, rates, and quantities of clearance of compounds from CSF or ISF to lymph, spinal cord, or

nasal tissue are affected by rate of infusion of fluid into a ventricle, the position of the subject (head up or down), and the molecular weight (size) of the substance [28, 87]. Brain disorders that alter glucose metabolism are also anticipated to influence metabolic water production and clearance rates, e.g., regional increases and decreases in CMR_{glc} during and after spreading cortical depression [96], reduced CMR_{glc} in Alzheimer's Disease [97], metabolic heterogeneity of glioblastoma brain tumors [98], traumatic brain injury [99], and other conditions.

A large fraction of metabolic water is generated by neuronal ATP synthase (28 of 38 H_2O/glucose) and is probably linked to ATP turnover, which is related to energy consuming processes of different components of excitatory signaling in the grey matter [100]. This relationship involves efflux of water from mitochondria to cytoplasm where it is consumed in hydrolytic reactions of cation pumps. On the other hand, metabolic water generated during rest by glycolysis, TCA cycle, and electron transport, i.e., 10 H_2O per glucose oxidized, is probably exported from brain cells where it may contribute to perivascular fluid and local water fluxes. Less metabolic water is generated during rises in activity due to upregulation of nonoxidative metabolism of glucose by neurons and of glycogen by astrocytes in activated brain regions. However, calculated release of water bound to glycogen during activation exceeds resting metabolic water secretion rate and may contribute to perivascular fluid fluxes and rapid perivascular lactate clearance Fig.7 . These are important topics for future study, and outstanding questions remain to be addressed:

- The metabolic basis of metabolic water production in the brain is incompletely understood, but secretion may occur at the same rate as the production of brain interstitial fluid (ISF). We provide here a set of guidelines for calculating water production when the rates of oxidative and non-oxidative metabolism of glucose and glycogen are known. Secretion of metabolic water into the ISF results in an outward flow of fluid, but do cerebrospinal fluid and metabolic water mix within the ISF and, if so, does this vary with activity, e.g. awake rest versus deep sleep?
- There are currently no methods that can be used to measure local metabolic water production in the intact brain. One question is whether we can develop methods to record metabolic water fluxes in the living human and rodent brain. If so, can metabolic water be evaluated as a driver of fluid flow from the brain through the perivascular-lymphatic system?
- The amount of water bound to astrocytic glycogen and the ratio of bound water to glucosyl units in glycogen at different glycogen concentrations are not known. Can we develop methods to measure glycogen-bound water and its release as glycogen is degraded?
- Mitochondria in neurons are expected to release most of the metabolic water, but can we develop methods to distinguish between astrocyte and neuronal sources of water at rest and during increases in activity?
- Glycogen is rapidly metabolized by non-oxidative metabolism during increases in activity, leading to lactate release. Does glycogen-bound water help remove lactate produced by glycogen metabolism?
- Does metabolic water contribute to unrecognized sources of cerebrospinal fluid in disease states, e.g. hydrocephalus or oedema formation?
- Does metabolic water production during brain development involve oxidation of alternative substrates, including lactate, ketone bodies (β-hydroxybutyrate and acetoacetate), and other compounds (see Table 2 in [101])?
- Does lipid metabolism in demyelinating diseases contribute to brain water production?
- Neuronal mitochondria produce the majority of metabolic water and its production should be affected by mitochondrial dysfunction, hypoxia, anoxia and ischemia. Is metabolic water production altered by mitochondrial diseases and disorders?

Limitations and future directions

A limitation of this study is that the metabolic water produced by different pathways was calculated using the established mechanistic stoichiometry of enzymatic reactions of glucose metabolism, rather than in vivo experimental data produced by the authors themselves. Nevertheless, our calculations are founded upon established experimental evidence that corroborates the attribution of cellular contributions to the formation of metabolic water during periods of rest and activation. Future metabolic studies in awake resting and stimulated rats and humans, including glycogen consumption, are needed to improve the accuracy of calculated metabolic water production rates in neurons and astrocytes. In addition, the calculated amounts and cell types producing metabolic water under different conditions in this study can serve as a blueprint for design and anticipated results of studies to measure metabolic water production. Taken together, our findings implicate metabolic water production by neurons and astrocytes as an essential element of brain fluid homeostasis, a discovery with broad

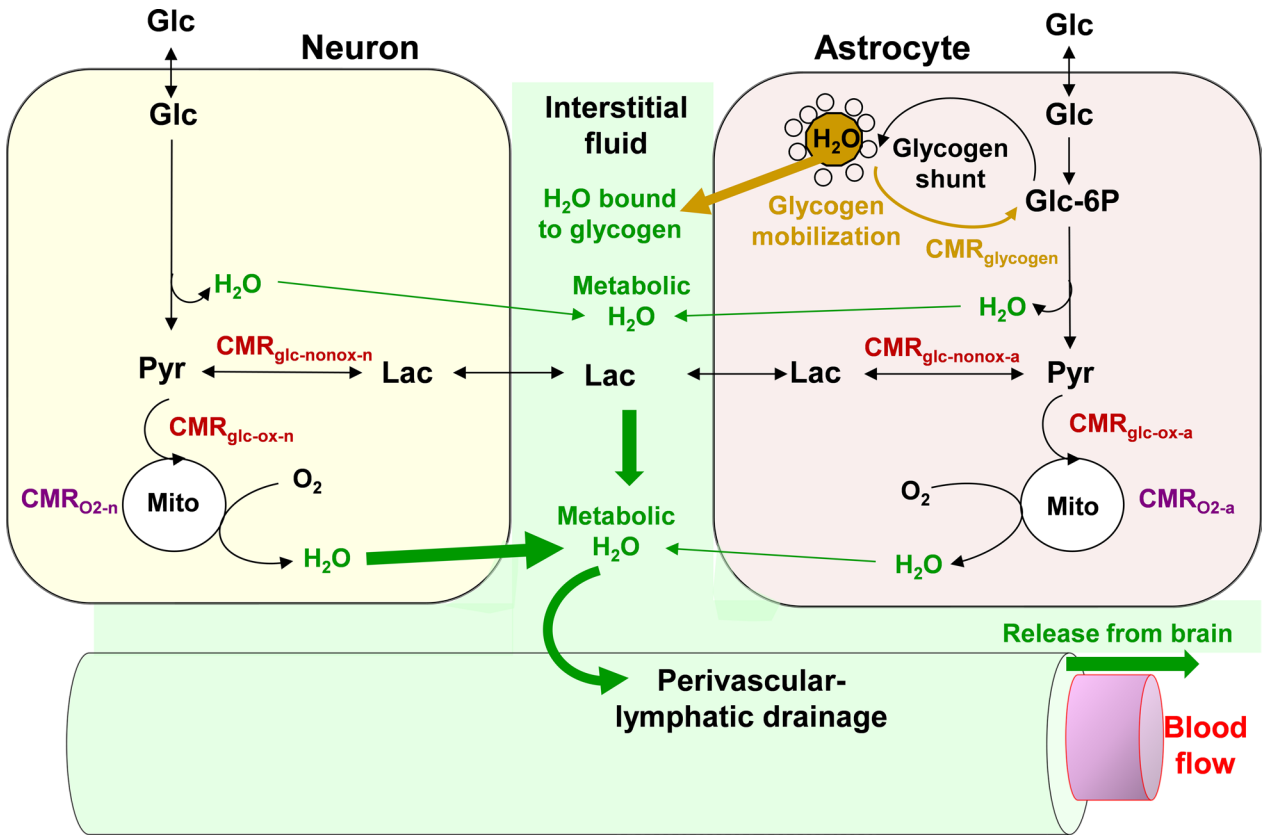

Fig. 7 Overview of the major aspects of metabolic water budget. Oxidation of glucose, the obligatory brain fuel, continuously produces metabolic water that is secreted to interstitial fluid and contributes to perivascular-lymphatic drainage. Neuronal mitochondria generate most metabolic water. More metabolic water is produced during rest than during stimulation and deep sleep when glucose oxidation is reduced, but astrocytic glycogen breakdown during activation is anticipated to release bound water that may be a driver of fluid flow and waste clearance. Metabolic and bound water impact fluid dynamics in healthy and diseased brains

implications for human brain health. On the one hand, our results have implications for the interpretation of brain fluid flow, suggesting that the relationship between brain fluids and ongoing and evoked neural activity is crucial for understanding the dynamics of brain interstitial fluid, which may be severely compromised in pathological contexts. On the other hand, modulation of neuronal and astrocytic metabolism may provide a therapeutic target to improve waste removal in the context of neurodegeneration, thereby reducing the accumulation of toxic proteins thought to drive disease progression.

Appendix

Reactions that consume and produce water during metabolism of glucose

Figure 8 illustrates the pathways of glucose metabolism that produce and consume water, and Table 2 provides details of each of the reactions of glucose metabolism.

Metabolic water during metabolism of Glc-6P via branch pathways

Alternative fates of Glc-6-P

Glc-6P is metabolized in the pentose phosphate pathway (PPP) to produce NADPH for management of oxidative stress and biosynthetic reactions, it is converted into glycogen as an astrocytic energy reserve that is mobilized during activation, and used for synthesis of complex carbohydrates. Glc-6-phosphatase is present in brain and would consume water ($Glc\text{-}6P + H_2O \rightarrow Glc + Pi$), but its activity is very low [102] (vs. liver). Glc-6-phosphatase may, in fact, have a separate, neuroprotective role, i.e., to hydrolyze a toxic metabolite, 1,5-anhydroglucitol-6-P [103]. 1,5-Anhydroglucitol is present in various foods and after ingestion it can be phosphorylated by hexokinase and accumulate to toxic levels [104, 105].

Pentose-P pathway (PPP)

In the first step of the PPP, 1 Glc-6P, 2 $NADP^+$ and 1 H_2O are consumed to produce 2 $NADPH + 2\ H^+ + 1\ CO_2$ + ribulose-5P (Fig. 8), whereas the other PPP

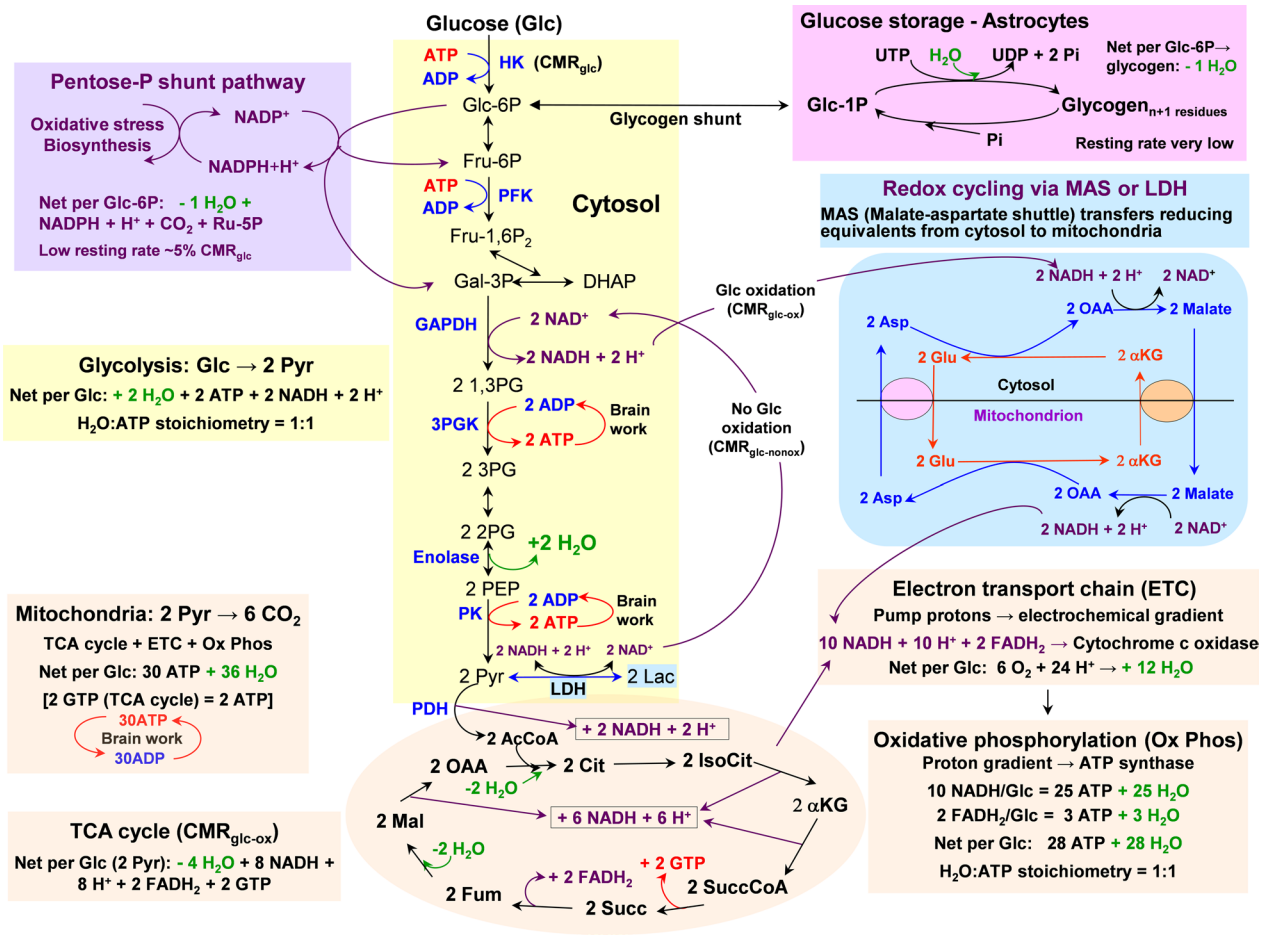

Fig. 8 Major pathways of glucose metabolism involved in production and consumption of metabolic water. (Related to Main text Sect. "Metabolic water production during glucose metabolism in resting, awake, non-stimulated subjects" and Figs. 1–4) Details of the major (glycolytic pathway [yellow background color] and TCA cycle, electron transport chain, and oxidative phosphorylation [pink background color]) and minor (pentose shunt pathway and glycogen storage) sites of metabolic water production and consumption during metabolism of glucose. Under the resting, awake, non-stimulated condition, nearly all of the glucose is oxidized and the cytosolic NADH is shuttled to the mitochondria via the malate-aspartate shuttle (blue background). When glucose (Glc) is completely oxidized it is converted to 2 pyruvate (Pyr) by the glycolytic pathway, and the reducing equivalents are shuttled to the mitochondrial electron transport chain (ETC) via the malate-aspartate shuttle (MAS). Oxidation of 2 Pyr in the tricarboxylic acid (TCA) cycle generates NADH + H^+ + $FADH_2$ that enter the ETC and produce metabolic water at the cytochrome c oxidase step. Oxidative phosphorylation uses the proton gradient generated by the ETC to drive ATP synthase and produce ATP + metabolic H_2O. Branch pathways can divert glucose-6-phosphate (Glc-6P) into the pentose phosphate pathway (PPP) or to glycogen synthesis (predominantly in astrocytes) (See Sect. "Metabolic water during metabolism of Glc-6P via branch pathways"). The first step of the PPP consumes 1 H_2O per Glc-6P entering the pathway. Glycogen synthesis also consumes 1 H_2O per glucosyl unit added to the polymer. The rates of both of these pathways are low under resting, awake, non-stimulated conditions and their contributions to metabolic water balance are not included with those of the major pathways: glycolysis, TCA cycle, electron transport, and oxidative phosphorylation. During nonoxidative metabolism pyruvate is converted to lactate by lactate dehydrogenase to regenerate NAD^+ so that glycolytic flux can continue. This lactate is released from the cell, and pyruvate is removed as an oxidative substrate. Abbreviations: + denotes produced,—denotes consumed; Glc, glucose; Glc-6P, glucose-6-phosphate; P, phosphate; Fru-6P, fructose-6-P; Fru-1,6P_2, fructose-1,6-bisphosphate; Gal-3P, glyceraldehyde-3-P; GAPDH, glyceraldehyde-3P dehydrogenase; DHAP, dihydroxyacetone phosphate; Pi, inorganic phosphate (HPO_4^{-2}); 1,3PG, 1,3-bisphosphoglycerate; 3PG, 3-phosphoglycerate; 2-PG, 2-phosphoglycerate; PEP, phosphoenolpyruvate; Pyr, pyruvate; Lac, lactate; AcCoA, Acetyl Coenzyme A; OAA, oxaloacetate; cit, citrate; isocit, isocitrate; αKG, α-ketoglutarate; SuccCoA, succinyl CoA; succ, succinate; Fum, fumarate; mal, malate; Asp, aspartate; MAS, malate-aspartate shuttle; LDH, lactate dehydrogenase; Ru-5P, ribulose-5-phosphate; TCA, tricarboxylic acid; HK, hexokinase; PFK, phosphofructokinase; GAPDH, glyceraldehyde-3-phosphate dehydrogenase; 3PGK, 3-phosphoglycerate kinase; PDH, pyruvate dehydrogenase; CMR_{glc}, cerebral metabolic rate of glucose utilization; $CMR_{glc\text{-}ox}$, cerebral metabolic rate of glucose oxidation. Modified from Fig. 1 in Dienel [13], Copyright © 2019, The American Physiological Society

reactions do not involve water (Table 2). Metabolism of three Glc-6P molecules via the PPP produces 3 CO_2 plus 2 fructose-6P (Fru-6P) + 1 glyceraldehyde-3-phosphate (Gal-3P) (Table 2), and the latter two metabolites can re-enter the glycolytic pathway. Due to the decarboxylation step that removes the equivalent of one triose from 3 Glc-6P (compare Table 2), the net yields of H_2O, ATP, and NADH + H^+ via the PPP plus glycolysis and oxidation per glucose phosphorylated are lower than for direct glucose oxidation. PPP flux in awake, unstimulated subjects is only ~ 5% of glycolytic flux [13], and its contribution to metabolic water was ignored. However, during brain activation, PPP flux can increase and rise to 20–25% of glycolytic flux in vivo [39, 106] causing the PPP to consume more water at the Glc-6-P dehydrogenase step and produce less water via oxidation. Thus, the impact of PPP flux on metabolic water balance is highest during activation, oxidative stress, or nucleotide biosynthesis.

Glycogen turnover

Rodent brain contains high amounts of glycogen, 10–12 µmol/g (expressed as glucose equivalents) versus 2–3 µmol/g for glucose [107, 108], and it is mobilized during activation [44, 109–111]. Most glycogen is located in astrocytes, but small amounts are present in neurons [112, 113]. Glycogen turnover in the awake, unstimulated rodent and human brain is low, and small amounts of label from blood-borne glucose are incorporated into glycogen during rest, activation, and recovery [111, 114–116].

During glycogen synthesis, water and ATP equivalents (UDP + ATP ↔ UTP + ADP) are consumed (Table 2), but the amount is minimal in the resting state and is not included in the metabolic water summary. Glycogen phosphorylase produces Glc-1P that is converted to Glc-6P by phosphoglucomutase (Table 2). Glycogen phosphorylase does not involve water, nor do the glycogen branching and debranching steps (not shown in Table 2). However, ~ 10% of the glucosyl residues in glycogen are released as glucose because the debranching enzyme also has glucosidase activity and hydrolyzes (consumes 1 H_2O) the α (1 → 6) bond of the residue that remains at the branch point after debranching. Water is involved in reactions that relate to allosteric control of glycogen turnover, e.g., protein phosphatases, adenylate cyclase-pyrophosphatase (ATP → cAMP + PPi; PPi + H_2O → 2Pi; PPi = pyrophosphate), and phosphodiesterase (cAMP + H_2O → AMP), whereas protein kinase A utilizes phosphoryl transfer, not water. Water usage in these regulatory processes is not included with glucose metabolic water.

During activation, glycogenolysis generates Glc-6P that enters the glycolytic pathway downstream of the hexokinase step and does not consume ATP until the phosphofructokinase step, resulting in a 50% higher glycolytic ATP yield than from glucose, 3 versus 2 ATP. If the Glc-6P is metabolized to 2 pyruvate, the yield of 2 H_2O and 2 NADH + 2 H^+ is the same as glucose (Fig. 8, Table 2), whereas if converted to 2 lactate, the 2 NADH + 2 H^+ are consumed to regenerate 2 NAD^+ and metabolic water production by astrocytic oxidation is eliminated (Fig. 8).

Summary

Water is consumed by the first step of the pentose phosphate pathway (Fig. 8, Table 2), but during resting conditions the rate is very low and can be neglected. PPP flux increases during activation and it will reduce net metabolic water production. Glycogen synthesis also consumes water (Fig. 8, Table 2), but its rate is low and can be omitted from metabolic water balance. Mobilization of glycogen does not involve water, but metabolic water is produced from glycogen-derived Glc-6P metabolism via the glycolytic pathway and glycogenolysis is anticipated to release its bound water that may contribute to water efflux from astrocytes (Fig. 7).

Discordant metabolic water amounts: calorimetric versus enzymatic glucose oxidation

Horiike et al. [117] addressed the apparent discrepancy in the net amount of water formed if glucose metabolism is uncoupled from ATP synthesis (10 H_2O for glycolysis + TCA cycle + electron transport) and that from calorimetry mass balance (6 H_2O). They explained the 'excess' 4 water in terms of the resonance structures of Pi = HPO_4^{-2} ↔ [OH^-] + [+P O_3^{-2}], where the [OH^-] is equivalent to water (*but not a water molecule* in the actual reaction mechanisms), with net consumption of 1 H_2O equivalent as [OH^-] per substrate-level phosphorylation reaction, i.e., −2 for the overall glyceraldehyde-3P dehydrogenase (GAPDH) + phosphoglycerate kinase reaction and −2 for succinyl-CoA synthetase reaction, both per glucose oxidized. In these reaction mechanisms, Horiike et al. [117] noted that the [O −] from Pi constitutes the [O −] of the $-COO^-$ group of the product (either 3P-glycerate or succinate, respectively) and [+PO_3^{-2}] is transferred to ADP or GDP. This mechanistic interpretation results in no net water formed via glycolysis (i.e., + 2 H_2O from enolase and −2 [OH^-] from GAPDH + 3P-glycerate

kinase) and net of 6 consumed in the TCA cycle (−2 H_2O citrate synthase, −2 H_2O fumarase, and −2 [OH-] succinyl CoA synthetase). With the electron transport chain-mediated production of +12 H_2O minus 4 H_2O and minus 2 [OH-] consumed in the TCA cycle and net zero H_2O in the glycolytic pathway yields a net of +6 H_2O produced per glucose, in agreement with the mass balance Eq. (1). Mechanistically, the dual role of Pi as a water substitute plus phosphoryl donor can balance the stoichiometry of biological oxidation of glucose versus calorimetric oxidation, but the former generates a net of 10 H_2O molecules via the enzymatic reactions (Figs. 2, 8, Table 2).

The mechanistic interpretation of glucose oxidation stoichiometry by Horiike et al. [117] was challenged by Mitchell [118], and in their rebuttal, Horiike et al. [119] noted that their concept was mis-understood (lactate production is irrelevant) and explained that the water produced by ATP synthase will vary with the P/O ratio used in the oxidative phosphorylation calculation, which was 3 and 2 for $NADH + H^+$ and $FADH_2$, respectively, in their calculations versus 2.5 and 1.5, respectively, in Table 2 [34]. This will influence the total amount of water formed per glucose but not the apparent discrepancy of the 4 H_2O excess produced by the biological reactions compared to calorimetry (Table 2).

Evidence for disproportionate rise in nonoxidative metabolism during activation

The following material provides additional evidence to support the discussion in the main text of preferential upregulation of glycolysis when brain activity is increased during mental work, physical exercise, or sensory stimulation).

Parallel assays with [^{14}C]deoxyglucose (DG) and [1- or 6-^{14}C] glucose

These studies revealed that CMR_{glc} determined with [^{14}C]glucose underestimated CMR_{glc} by ~ 50% compared with rates determined with [^{14}C]DG [39, 40, 43, 111, 120]. [^{14}C]DG measures total CMR_{glc} at the hexokinase step [26] (Figs. 1, 8), and metabolites of [^{14}C]DG, mainly [^{14}C]DG-6P, are retained in the cells where the [^{14}C]DG was phosphorylated. The reason CMR_{glc} was too low in [^{14}C]glucose assays during activation is that trapping of the ^{14}C in the metabolite pools was incomplete due to rapid efflux of labeled lactate from brain to blood and perivascular fluid. Thus, metabolic assays during activation using [^{14}C- or ^{13}C]glucose will substantially underestimate total CMR_{glc} and nonoxidative glucose utilization during activation and upregulation of glycolysis.

Global metabolic assays by arteriovenous difference

During representative activation studies, the ratio of CMR_{O2}/CMR_{glc} (called the oxygen-glucose index, OGI), calculated from measured arteriovenous (AV) differences across the brain for oxygen and glucose (AV_{O2}/AV_{glc}), fell from the resting value of ~ 6 to ~ 5 during sensory stimulation of the rat [110] and to as low as ~ 3 during exhaustive exercise in humans [121]. OGI decreases indicate upregulation of nonoxidative metabolism of glucose compared with oxygen, as observed in the above studies with labeled glucose and DG. Lactate is an important supplemental oxidative fuel during exhaustive exercise due to large increases blood lactate concentrations [122, 123], and its oxidation would contribute to metabolic water production. Nevertheless, in spite of lactate oxidation, the oxygen/carbohydrate and oxygen/glucose indicies fall during exhaustive exercise, and the fate of the lactate generated from glucose metabolism in brain remains to be determined [124].

Contribution of glycogenolysis to fall in oxygen-glucose index

Using 5 min sensory stimulation of rats, brain glycogen level fell from the resting level of 12.3–9.6 = 2.7 µmol/g consumed, giving a glycogenolysis rate of 2.7/5 = 0.54 µmol/g/min in astrocytes (Table 1), a rate equal to 58% of the corresponding CMR_{glc} in all brain cells, 0.93 µmol/g/min [111]. Notably, the brain lactate level rose from 0.6 to 1.7 = 1.1 µmol/g, only ~ 1/5th of the lactate equivalents of the glycogen consumed (2 × 2.7 = 5.4 µmol/g lactate) [111], consistent with rapid efflux of glycogen-derived lactate. Utilization of endogenous glycogen is not taken into account in AV assays of glucose and oxygen, but glycogen consumption measured in the same experimental paradigm as that in which AV differences were measured reduced the calculated OGI from 5 [110] to 2.8 [125], consistent with release of glycogen-derived lactate, not its oxidation.

Fate of lactate produced during activation

The above experiments rule out retention of glycogen-derived lactate in the brain and its oxidation within brain. Nevertheless, if the possibility were considered that the glycogen-derived lactate were transferred to neurons or other astrocytes and oxidized, the OGI would, instead of falling to 2.8, rise above the theoretical maximal value of 6 *during activation* because Glc-6P from glycogen would be oxidized, consuming even more oxygen than blood-borne glucose alone. Furthermore, the specific activity (^{14}C dpm/µmole) of lactate purified from brain extracts during rest, activation and recovery was always about half that of [1- or 6-^{14}C]glucose (because only one of the

two lactate is labeled) [126], indicating that (i) blood-borne [^{14}C]glucose is the source of the [^{14}C]lactate purified from brain extracts, and (ii) unlabeled lactate derived from glycogen did not dilute the specific activity of the [^{14}C]lactate recovered from the brain. If the unlabeled glycogen-derived lactate remained in the brain, it would mix with the ^{14}C-labeled lactate during extract preparation and reduce its specific activity. These findings are consistent with compartmentation of nonoxidative glycolytic metabolism blood-borne [^{14}C]glucose in neurons in vivo and glycolytic metabolism of unlabeled glycogen in astrocytes. These findings are supported by the demonstration that activated cultured neurons increase glycolysis to produce and release lactate; they do not oxidize extracellular lactate [127, 128].

Neurovascular coupling model

Activation also causes the disproportionate upregulation of cerebral blood flow (CBF) and CMR_{glc} relative to CMR_{O2} (neurovascular coupling), and an AV flux balance model was recently developed to evaluate simultaneous homeostasis of pH, pCO_2, and pO_2. The model-predicted results were similar to experimental values, supporting the conclusion that the CBF-CMR_{O2} relationship is due to proton (and lactate) production by increased nonoxidative glycolysis and glycogenolysis, with clearance by CBF [129]. The lactate-proton clearance predictions of the neurovascular coupling model suggest that the perivascular clearance route is necessary because increases in blood lactate concentration during various physiological conditions (e.g., physical activity [33]) can rise higher than that in brain and impair the concentration gradient-dependent efflux of lactate from brain to blood during activation [129].

Alternative substrates and routes for water fluxes associated with metabolism

Supplemental fuels

Glucose is the major, obligatory fuel for resting and activated brain in sedentary subjects, but under various conditions, supplemental fuels can also be consumed to produce metabolic water and ATP. For example, lactate level in blood rises during extreme exercise, enters the brain, and is oxidized [123], perhaps sparing glucose for glycolysis to support ion pumping. During starvation or with high-fat diets, blood levels of ketone bodies increase, enter brain, and are oxidized [130]. After transamination, different amino acids can be oxidized in the TCA cycle [17].

Aquaporins

Glucose utilization is higher in neurons than in astrocytes (calculated per gram tissue, but not when adjusted for astrocyte volume fraction [52]), and the energy demands of specific cellular components differ among excitatory and inhibitory neurons and glia [21]. Neuronal glucose and water fluxes are greater than in astrocytes, and excitatory neurons have the highest CMR_{glc} [21] and produce most of the metabolic water.

This raises the question of how water exits neurons—perhaps metabolic water crosses the neuronal plasma membrane in conjunction with local extracellular osmotic changes, but this is incompletely understood. Astrocytes express aquaporin 4 as their predominant water channel, whereas aquaporins are sparse in most neurons [2, 131]. Water can cross the BBB, but its movement is not entirely free but rather tightly regulated by various physiological mechanisms [88, 132]. The tight junctions between the brain's endothelial cells prevent the movement of ions and can be thought of as a semipermeable membrane that allows an osmotic pressure gradient to build up, opposing or facilitating the movement of water from the blood into the brain and vice versa.

Metabolite transporters

Glucose transporters (GLUTs) are present in capillaries and all brain cells. GLUT1 is primarily in the endothelium and astrocytes and GLUT3 is primarily in neurons [133]. GLUT1, GLUT2, and GLUT3 have been reported to have water channel properties, with water fluxes driven by osmotic changes [62, 134–138]. The regional densities of GLUT1 and GLUT3 immunoreactive protein correlate with local capillary densities, glucose transport rates, and glucose utilization rates [139–141] indicating that any water fluxes through GLUTs may parallel metabolic demand and glucose metabolism to produce metabolic water. In addition, other metabolite transporters, including the monocarboxylic acid transporter MCT1 for lactate, co-transport water along with their substrates [56, 57, 59]. The contributions of transporter-mediated water fluxes to perivascular fluid, if any, are not known. These fluxes may be associated with changes in glucose utilization and cellular activity, but they are not metabolic water.

Abbreviations

AV	Arteriovenous
BBB	Blood-brain barrier
CMR_{glc}	Cerebral metabolic rate of glucose utilization
CMR_{O2}	Cerebral metabolic rate of oxygen utilization
CSF	Cerebrospinal fluid
ECF	Extracellular fluid

ECS	Extracellular space
ETC	Electron transport chain
Glc	Glucose
Glc-6P	Glucose-6-phosphate
GSG	Glucose sparing by glycogenolysis
ISF	Interstitial fluid
MRS	Magnetic resonance spectroscopy
OGI	Oxygen-glucose index = CMR_{O2}/CMR_{glc}
Pi	Inorganic phosphate
TCA	Tricarboxylic acid

Acknowledgements
None.

Author contributions
Both authors (GAD and ML) were involved in the development of the concepts, analysis of the data, and preparation of the manuscript. Both authors read and approved the final version of the manuscript.

Funding
Open access funding provided by Copenhagen University. This work was supported by the Lundbeck Foundation (#R392-2018-2266, #R345-2020-1440).

Data availability
The data sets that support the conclusions of this article are included in the article by referencing the papers from which the data were extracted.

Declarations

Ethics approval and consent to participate
Not applicable.

Consent for publication
We agree to the terms of the BioMed Central Copyright and License Agreement as well as the article-processing charge (APC) that applies for each article accepted for publication in *Fluids and Barriers of the CNS*.

Competing interest
The authors declare no competing interests.

Received: 15 December 2024 Accepted: 27 March 2025
Published online: 06 May 2025

References

1. MacAulay N. Molecular mechanisms of brain water transport. Nat Rev Neurosci. 2021;22(6):326–44.
2. Nagelhus EA, Ottersen OP. Physiological roles of aquaporin-4 in brain. Physiol Rev. 2013;93(4):1543–62.
3. Nicholson C. Dynamics of the brain cell microenvironment. Neurosci Res Program Bull. 1980;18(2):175–322.
4. Thorne RG, Nicholson C. In vivo diffusion analysis with quantum dots and dextrans predicts the width of brain extracellular space. Proc Natl Acad Sci USA. 2006;103(14):5567–72.
5. Holter KE, Kehlet B, Devor A, Sejnowski TJ, Dale AM, Omholt SW, et al. Interstitial solute transport in 3D reconstructed neuropil occurs by diffusion rather than bulk flow. Proc Natl Acad Sci USA. 2017;114(37):9894–9.
6. Aspelund A, Antila S, Proulx ST, Karlsen TV, Karaman S, Detmar M, et al. A dural lymphatic vascular system that drains brain interstitial fluid and macromolecules. J Exp Med. 2015;212(7):991–9.
7. Louveau A, Smirnov I, Keyes TJ, Eccles JD, Rouhani SJ, Peske JD, et al. Structural and functional features of central nervous system lymphatic vessels. Nature. 2015;523(7560):337–41.
8. Mestre H, Mori Y, Nedergaard M. The Brain's glymphatic system: current controversies. Trends Neurosci. 2020;43(7):458–66.
9. Kutuzov N, Flyvbjerg H, Lauritzen M. Contributions of the glycocalyx, endothelium, and extravascular compartment to the blood-brain barrier. Proc Natl Acad Sci USA. 2018;115(40):E9429–38.
10. Albargothy NJ, Johnston DA, MacGregor-Sharp M, Weller RO, Verma A, Hawkes CA, et al. Convective influx/glymphatic system: tracers injected into the CSF enter and leave the brain along separate periarterial basement membrane pathways. Acta Neuropathol. 2018;136(1):139–52.
11. Bakker EN, Bacskai BJ, Arbel-Ornath M, Aldea R, Bedussi B, Morris AW, et al. Lymphatic clearance of the brain: perivascular, paravascular and significance for neurodegenerative diseases. Cell Mol Neurobiol. 2016;36(2):181–94.
12. Abbott NJ, Pizzo ME, Preston JE, Janigro D, Thorne RG. The role of brain barriers in fluid movement in the CNS: Is there a 'glymphatic' system? Acta Neuropathol. 2018;135(3):387–407.
13. Dienel GA. Brain glucose metabolism: integration of energetics with function. Physiol Rev. 2019;99(1):949–1045.
14. Sokoloff L. Metabolism of the central nervous system in vivo. In: Field J, Magoun HW, Hall VE, editors. Handbook of Physiology - Neurophysiology. 3. Washington, DC: American Physiological Society; 1960. p. 1843–64.
15. Siesjö BK. Brain energy metabolism. Chichester: Wiley; 1978.
16. Erecinska M, Silver IA. ATP and brain function. J Cereb Blood Flow Metab. 1989;9(1):2–19.
17. Voet D, Voet JG, Pratt CW. Fundamentals of Biochemistry: Life at the Molecular Level, 5th Edition. Wiley; 2016.
18. Kimelberg HK. Water homeostasis in the brain: basic concepts. Neuroscience. 2004;129:851–60.
19. Rapoport SI. Blood-brain barrier in physiology and medicine New York: Raven Press; 1976.
20. Hall CN, Klein-Flugge MC, Howarth C, Attwell D. Oxidative phosphorylation, not glycolysis, powers presynaptic and postsynaptic mechanisms underlying brain information processing. J Neurosci. 2012;32(26):8940–51.
21. Yu Y, Herman P, Rothman DL, Agarwal D, Hyder F. Evaluating the gray and white matter energy budgets of human brain function. J Cereb Blood Flow Metab. 2018;38(8):0339–1353.
22. Nafstad PH, Blackstad TW. Distribution of mitochondria in pyramidal cells and boutons in hippocampal cortex. Z Zellforsch Mikrosk Anat. 1966;73(2):234–45.
23. Chavan V, Willis J, Walker SK, Clark HR, Liu X, Fox MA, et al. Central presynaptic terminals are enriched in ATP but the majority lack mitochondria. PLoS ONE. 2015;10(4): e0125185.
24. Shepherd GM, Harris KM. Three-dimensional structure and composition of CA3–>CA1 axons in rat hippocampal slices: implications for presynaptic connectivity and compartmentalization. J Neurosci. 1998;18(20):8300–10.
25. Derouiche A, Haseleu J, Korf HW. Fine astrocyte processes contain very small mitochondria: glial oxidative capability may fuel transmitter metabolism. Neurochem Res. 2015;40(12):2402–13.
26. Sokoloff L, Reivich M, Kennedy C, Des Rosiers MH, Patlak CS, Pettigrew KD, et al. The [^{14}C]deoxyglucose method for the measurement of local cerebral glucose utilization: theory, procedure, and normal values in the conscious and anesthetized albino rat. J Neurochem. 1977;28(5):897–916.
27. Szentistvanyi I, Patlak CS, Ellis RA, Cserr HF. Drainage of interstitial fluid from different regions of rat brain. Am J Physiol. 1984;246(6 Pt 2):F835–44.
28. Bradbury MWB, Cserr HF. Drainage of cerebral interstitial fluid and of cerebrospinal fluid into lymphatics. In: Johnston MG, editor. Experimental biology of the lymphatic circulation. Research monographs in cell and tissue physiology. New York: Elsevier; 1985. p. 355–94.
29. Sokoloff L. Localization of functional activity in the central nervous system by measurement of glucose utilization with radioactive deoxyglucose. J Cereb Blood Flow Metab. 1981;1(1):7–36.
30. Liu G, Ladrón-de-Guevara A, Izhiman Y, Nedergaard M, Du T. Measurements of cerebrospinal fluid production: a review of the limitations and advantages of current methodologies. Fluids Barr CNS. 2022;19(1):101.
31. Dienel GA, Cruz NF. Aerobic glycolysis during brain activation: adrenergic regulation and influence of norepinephrine on astrocytic metabolism. J Neurochem. 2016;138(1):14–52.

32. Madsen PL, Hasselbalch SG, Hagemann LP, Olsen KS, Bulow J, Holm S, et al. Persistent resetting of the cerebral oxygen/glucose uptake ratio by brain activation: evidence obtained with the Kety-Schmidt technique. J Cereb Blood Flow Metab. 1995;15(3):485–91.
33. Dalsgaard MK. Fuelling cerebral activity in exercising man. J Cereb Blood Flow Metab. 2006;26(6):731–50.
34. Hinkle PC. P/O ratios of mitochondrial oxidative phosphorylation. Biochim Biophys Acta. 2005;1706(1–2):1–11.
35. Morth JP, Pedersen BP, Buch-Pedersen MJ, Andersen JP, Vilsen B, Palmgren MG, et al. A structural overview of the plasma membrane Na+, K+-ATPase and H+-ATPase ion pumps. Nat Rev Mol Cell Biol. 2011;12(1):60–70.
36. Lei H, Ugurbil K, Chen W. Measurement of unidirectional Pi to ATP flux in human visual cortex at 7 T by using in vivo 31P magnetic resonance spectroscopy. Proc Natl Acad Sci USA. 2003;100(24):14409–14.
37. Du F, Zhu XH, Zhang Y, Friedman M, Zhang N, Ugurbil K, et al. Tightly coupled brain activity and cerebral ATP metabolic rate. Proc Natl Acad Sci USA. 2008;105(17):6409–14.
38. Dienel GA. Brain lactate metabolism: the discoveries and the controversies. J Cereb Blood Flow Metab. 2012;32(7):1107–38.
39. Dienel GA. Fueling and imaging brain activation. ASN Neuro. 2012;4(5):267–321. art:e00093. https://doi.org/10.1042/AN20120021
40. Cruz NF, Adachi K, Dienel GA. Rapid efflux of lactate from cerebral cortex during K+ -induced spreading cortical depression. J Cereb Blood Flow Metab. 1999;19(4):380–92.
41. Ball KK, Cruz NF, Mrak RE, Dienel GA. Trafficking of glucose, lactate, and amyloid-beta from the inferior colliculus through perivascular routes. J Cereb Blood Flow Metab. 2010;30(1):162–76.
42. Gandhi GK, Cruz NF, Ball KK, Dienel GA. Astrocytes are poised for lactate trafficking and release from activated brain and for supply of glucose to neurons. J Neurochem. 2009;111(2):522–36.
43. Adachi K, Cruz NF, Sokoloff L, Dienel GA. Labeling of metabolic pools by [6-^{14}C]glucose during K(+)-induced stimulation of glucose utilization in rat brain. J Cereb Blood Flow Metab. 1995;15(1):97–110.
44. Swanson RA. Physiologic coupling of glial glycogen metabolism to neuronal activity in brain. Can J Physiol Pharmacol. 1992;70(Suppl):S138–44.
45. DiNuzzo M, Mangia S, Maraviglia B, Giove F. The role of astrocytic glycogen in supporting the energetics of neuronal activity. Neurochem Res. 2012;37:2432–8.
46. Rothman DL, Dienel GA, Behar KL, Hyder F, DiNuzzo M, Giove F, et al. Glucose sparing by glycogenolysis (GSG) determines the relationship between brain metabolism and neurotransmission. J Cereb Blood Flow Metab. 2022;42(5):844–60.
47. Cornford EM, Hyman S, Swartz BE. The human brain GLUT1 glucose transporter: ultrastructural localization to the blood-brain barrier endothelia. J Cereb Blood Flow Metab. 1994;14(1):106–12.
48. Cornford EM, Nguyen EV, Landaw EM. Acute upregulation of blood-brain barrier glucose transporter activity in seizures. Am J Physiol Heart Circ Physiol. 2000;279(3):H1346–54.
49. Ashrafi G, Ryan TA. Glucose metabolism in nerve terminals. Curr Opin Neurobiol. 2017;45:156–61.
50. Ashrafi G, Wu Z, Farrell RJ, Ryan TA. GLUT4 mobilization supports energetic demands of active synapses. Neuron. 2017;93(3):606-15.e3.
51. Kadekaro M, Crane AM, Sokoloff L. Differential effects of electrical stimulation of sciatic nerve on metabolic activity in spinal cord and dorsal root ganglion in the rat. Proc Natl Acad Sci USA. 1985;82(17):6010–3.
52. Dienel GA, Rothman DL. Reevaluation of astrocyte-neuron energy metabolism with astrocyte volume fraction correction: impact on cellular glucose oxidation rates, glutamate-glutamine cycle energetics, glycogen levels and utilization rates vs. exercising muscle, and Na(+)/K(+) pumping rates. Neurochem Res. 2020;45(11):2607–30.
53. Fernández-Elías VE, Ortega JF, Nelson RK, Mora-Rodriguez R. Relationship between muscle water and glycogen recovery after prolonged exercise in the heat in humans. Eur J Appl Physiol. 2015;115(9):1919–26.
54. Shiose K, Takahashi H, Yamada Y. Muscle glycogen assessment and relationship with body hydration status: a narrative review. Nutrients. 2022;15(1):155.
55. Shiose K, Yamada Y, Motonaga K, Sagayama H, Higaki Y, Tanaka H, et al. Segmental extracellular and intracellular water distribution and muscle glycogen after 72-h carbohydrate loading using spectroscopic techniques. J Appl Physiol. 2016;121(1):205–11.
56. MacAulay N, Zeuthen T. Water transport between CNS compartments: contributions of aquaporins and cotransporters. Neuroscience. 2010;168(4):941–56.
57. Zeuthen T. Water-transporting proteins. J Membr Biol. 2010;234(2):57–73.
58. Zeuthen T, Alsterfjord M, Beitz E, MacAulay N. Osmotic water transport in aquaporins: evidence for a stochastic mechanism. J Physiol. 2013;591(Pt 20):5017–29.
59. MacAulay N, Keep RF, Zeuthen T. Cerebrospinal fluid production by the choroid plexus: a century of barrier research revisited. Fluids Barr CNS. 2022;19(1):26.
60. Steffensen AB, Oernbo EK, Stoica A, Gerkau NJ, Barbuskaite D, Tritsaris K, et al. Cotransporter-mediated water transport underlying cerebrospinal fluid formation. Nat Commun. 2018;9(1):2167.
61. Zeuthen T, Zeuthen E, MacAulay N. Water transport by GLUT2 expressed in Xenopus laevis oocytes. J Physiol. 2007;579(2):345–61.
62. Naftalin RJ. Osmotic water transport with glucose in GLUT2 and SGLT. Biophys J. 2008;94(10):3912–23.
63. Schaeffer S, Iadecola C. Revisiting the neurovascular unit. Nat Neurosci. 2021;24(9):1198–209.
64. Krogsgaard A, Sperling L, Dahlqvist M, Thomsen K, Vydmantaite G, Li F, et al. PV interneurons evoke astrocytic Ca(2+) responses in awake mice, which contributes to neurovascular coupling. Glia. 2023;71(8):1830–46.
65. Cai C, Zambach SA, Grubb S, Tao L, He C, Lind BL, et al. Impaired dynamics of precapillary sphincters and pericytes at first-order capillaries predict reduced neurovascular function in the aging mouse brain. Nat Aging. 2023;3(2):173–84.
66. Hall CN, Reynell C, Gesslein B, Hamilton NB, Mishra A, Sutherland BA, et al. Capillary pericytes regulate cerebral blood flow in health and disease. Nature. 2014;508(7494):55–60.
67. Broggini T, Duckworth J, Ji X, Liu R, Xia X, Mächler P, et al. Long-wavelength traveling waves of vasomotion modulate the perfusion of cortex. Neuron. 2024;112(14):2349-67.e8.
68. Hirshkowitz M. Normal human sleep: an overview. The Medical clinics of North America. 2004;88(3):551–65, vii.
69. Boyle PJ, Scott JC, Krentz AJ, Nagy RJ, Comstock E, Hoffman C. Diminished brain glucose metabolism is a significant determinant for falling rates of systemic glucose utilization during sleep in normal humans. J Clin Invest. 1994;93(2):529–35.
70. Madsen PL, Vorstrup S. Cerebral blood flow and metabolism during sleep. Cerebrovasc Brain Metab Rev. 1991;3(4):281–96.
71. Buchsbaum MS, Gillin JC, Wu J, Hazlett E, Sicotte N, Dupont RM, et al. Regional cerebral glucose metabolic rate in human sleep assessed by positron emission tomography. Life Sci. 1989;45(15):1349–56.
72. Maquet P. Sleep function(s) and cerebral metabolism. Behav Brain Res. 1995;69(1–2):75–83.
73. Vyazovskiy VV, Harris KD. Sleep and the single neuron: the role of global slow oscillations in individual cell rest. Nat Rev Neurosci. 2013;14(6):443–51.
74. Saper CB, Fuller PM, Pedersen NP, Lu J, Scammell TE. Sleep state switching. Neuron. 2010;68(6):1023–42.
75. Xie L, Kang H, Xu Q, Chen MJ, Liao Y, Thiyagarajan M, et al. Sleep drives metabolite clearance from the adult brain. Science. 2013;342(6156):373–7.
76. Loredo JS, Nelesen R, Ancoli-Israel S, Dimsdale JE. Sleep quality and blood pressure dipping in normal adults. Sleep. 2004;27(6):1097–103.
77. Jukkola J, Kaakinen M, Singh A, Moradi S, Ferdinando H, Myllylä T, et al. Blood pressure lowering enhances cerebrospinal fluid efflux to the systemic circulation primarily via the lymphatic vasculature. Fluids Barr CNS. 2024;21(1):12.
78. Razzaghi Khamesi P, Charitatos V, Heerfordt EK, MacAulay N, Kurtcuoglu V. Are standing osmotic gradients the main driver of cerebrospinal fluid production? A computational analysis. Fluids Barr CNS. 2023;20(1):18.
79. Damkier HH, Brown PD, Praetorius J. Cerebrospinal fluid secretion by the choroid plexus. Physiol Rev. 2013;93:1847–92.
80. Bradbury MW, Kleeman CR. The effect of chronic osmotic disturbance on the concentrations of cations in cerebrospinal fluid. J Physiol. 1969;204(1):181–93.

81. Sykova E, Nicholson C. Diffusion in brain extracellular space. Physiol Rev. 2008;88:1277–340.
82. Johnston M, Papaiconomou C. Cerebrospinal fluid transport: a lymphatic perspective. News Physiol Sci. 2002;17:227–30.
83. Weller RO, Djuanda E, Yow HY, Carare RO. Lymphatic drainage of the brain and the pathophysiology of neurological disease. Acta Neuropathol. 2009;117(1):1–14.
84. Xiang J, Hua Y, Xi G, Keep RF. Mechanisms of cerebrospinal fluid and brain interstitial fluid production. Neurobiol Dis. 2023;183: 106159.
85. Abbott NJ. Evidence for bulk flow of brain interstitial fluid: significance for physiology and pathology. Neurochem Int. 2004;45:545–52.
86. Kipnis J. The anatomy of brainwashing. Science. 2024;385(6707):368–70.
87. Bradbury MW, Westrop RJ. Factors influencing exit of substances from cerebrospinal fluid into deep cervical lymph of the rabbit. J Physiol. 1983;339:519–34.
88. Hladky SB, Barrand MA. Mechanisms of fluid movement into, through and out of the brain: evaluation of the evidence. Fluids Barr CNS. 2014;11(1):1–32.
89. Rasmussen MK, Mestre H, Nedergaard M. Fluid transport in the brain. Physiol Rev. 2022;102(2):1025–151.
90. Hladky SB, Barrand MA. The glymphatic hypothesis: the theory and the evidence. Fluids Barriers CNS. 2022;19(1):9.
91. Wardlaw JM, Benveniste H, Nedergaard M, Zlokovic BV, Mestre H, Lee H, et al. Perivascular spaces in the brain: anatomy, physiology and pathology. Nat Rev Neurol. 2020;16(3):137–53.
92. Weller RO, Subash M, Preston SD, Mazanti I, Carare RO. Perivascular drainage of amyloid-beta peptides from the brain and its failure in cerebral amyloid angiopathy and Alzheimer's disease. Brain Pathol. 2008;18(2):253–66.
93. Carare RO, Bernardes-Silva M, Newman TA, Page AM, Nicoll JA, Perry VH, et al. Solutes, but not cells, drain from the brain parenchyma along basement membranes of capillaries and arteries: significance for cerebral amyloid angiopathy and neuroimmunology. Neuropathol Appl Neurobiol. 2008;34(2):131–44.
94. Jochems ACC, Blair GW, Stringer MS, Thrippleton MJ, Clancy U, Chappell FM, et al. Relationship between venules and perivascular spaces in sporadic small vessel diseases. Stroke. 2020;51(5):1503–6.
95. Hladky SB, Barrand MA. Regulation of brain fluid volumes and pressures: basic principles, intracranial hypertension, ventriculomegaly and hydrocephalus. Fluids Barriers CNS. 2024;21(1):57.
96. Shinohara M, Dollinger B, Brown G, Rapoport S, Sokoloff L. Cerebral glucose utilization: local changes during and after recovery from spreading cortical depression. Science. 1979;203(4376):188–90.
97. Herholz K, Salmon E, Perani D, Baron JC, Holthoff V, Frölich L, et al. Discrimination between Alzheimer dementia and controls by automated analysis of multicenter FDG PET. Neuroimage. 2002;17(1):302–16.
98. Simões RV, Henriques RN, Cardoso BM, Fernandes FF, Carvalho T, Shemesh N. Glucose fluxes in glycolytic and oxidative pathways detected in vivo by deuterium magnetic resonance spectroscopy reflect proliferation in mouse glioblastoma. NeuroImage Clin. 2022;33: 102932.
99. Mannino C, Glenn TC, Hovda DA, Vespa PM, McArthur DL, Van Horn JD, et al. Acute glucose and lactate metabolism are associated with cognitive recovery following traumatic brain injury. J Neurosci Res. 2017. https://doi.org/10.1002/jnr.24097.
100. Attwell D, Laughlin SB. An energy budget for signaling in the grey matter of the brain. J Cereb Blood Flow Metab. 2001;21(10):1133–45.
101. Benveniste H, Dienel G, Jacob Z, Lee H, Makaryus R, Gjedde A, et al. Trajectories of brain lactate and re-visited oxygen-glucose index calculations do not support elevated non-oxidative metabolism of glucose across childhood. Front Neurosci. 2018;12(631):631.
102. Dienel GA. The "protected" glucose transport through the astrocytic endoplasmic reticulum is too slow to serve as a quantitatively-important highway for nutrient delivery. J Neurosci Res. 2019;97(8):854–62.
103. Dienel GA. Hypothesis: a novel neuroprotective role for glucose-6-phosphatase (G6PC3) in brain-to maintain energy-dependent functions including cognitive processes. Neurochem Res. 2020;45(11):2529–52.
104. Wortmann SB, Van Hove JLK, Derks TGJ, Chevalier N, Knight V, Koller A, et al. Treating neutropenia and neutrophil dysfunction in glycogen storage disease IB with an SGLT2-inhibitor. Blood. 2020;136:1033–43.
105. Veiga-da-Cunha M, Chevalier N, Stephenne X, Defour JP, Paczia N, Ferster A, et al. Failure to eliminate a phosphorylated glucose analog leads to neutropenia in patients with G6PT and G6PC3 deficiency. Proc Natl Acad Sci USA. 2019;116(4):1241–50.
106. Ben-Yoseph O, Boxer PA, Ross BD. Noninvasive assessment of the relative roles of cerebral antioxidant enzymes by quantitation of pentose phosphate pathway activity. Neurochem Res. 1996;21(9):1005–12.
107. Cruz NF, Dienel GA. High glycogen levels in brains of rats with minimal environmental stimuli: implications for metabolic contributions of working astrocytes. J Cereb Blood Flow Metab. 2002;22(12):1476–89.
108. Oe Y, Baba O, Ashida H, Nakamura KC, Hirase H. Glycogen distribution in the microwave-fixed mouse brain reveals heterogeneous astrocytic patterns. Glia. 2016;64(9):1532–45.
109. Swanson RA, Morton MM, Sagar SM, Sharp FR. Sensory stimulation induces local cerebral glycogenolysis: demonstration by autoradiography. Neurosci. 1992;51(2):451–61.
110. Madsen PL, Cruz NF, Sokoloff L, Dienel GA. Cerebral oxygen/glucose ratio is low during sensory stimulation and rises above normal during recovery: excess glucose consumption during stimulation is not accounted for by lactate efflux from or accumulation in brain tissue. J Cereb Blood Flow Metab. 1999;19(4):393–400.
111. Dienel GA, Wang RY, Cruz NF. Generalized sensory stimulation of conscious rats increases labeling of oxidative pathways of glucose metabolism when the brain glucose-oxygen uptake ratio rises. J Cereb Blood Flow Metab. 2002;22(12):1490–502.
112. Duran J, Gruart A, Varea O, López-Soldado I, Delgado-García JM, Guinovart JJ. Lack of neuronal glycogen impairs memory formation and learning-dependent synaptic plasticity in mice. Front Cell Neurosci. 2019;13(374):1–11.
113. Duran J, Gruart A, López-Ramos JC, Delgado-García JM, Guinovart JJ. Glycogen in astrocytes and neurons: physiological and pathological aspects. Adv Neurobiol. 2019;23:311–29.
114. Watanabe H, Passonneau JV. Factors affecting the turnover of cerebral glycogen and limit dextrin in vivo. J Neurochem. 1973;20(6):1543–54.
115. Öz G, DiNuzzo M, Kumar A, Moheet A, Seaquist ER. Revisiting glycogen content in the human brain. Neurochem Res. 2015;40(12):2473–81.
116. DiNuzzo M. Kinetic analysis of glycogen turnover: relevance to human brain ^{13}C-NMR spectroscopy. J Cereb Blood Flow Metab. 2013;33(10):1540–8.
117. Horiike K, Miura R, Ishida T, Nozaki M. Stoichiometry of the water molecules in glucose oxidation revisited: inorganic phosphate plays a unique role as water in substrate-level phosphorylation. Biochem Educ. 1996;24(1):17–20.
118. Mitchell RA. Stoichiometry of glucose oxidation when linked to ATP synthesis. Biochem Educ. 1996;24(4):207–8.
119. Horiike K, Ishida T, Miura R. How many water molecules produce during the complete oxidation of glucose? Reply to Robert A Mitchell. Biochem Educ. 1996;24(4):208–9.
120. Dienel GA, Hertz L. Glucose and lactate metabolism during brain activation. J Neurosci Res. 2001;66(5):824–38.
121. Dalsgaard MK, Quistorff B, Danielsen ER, Selmer C, Vogelsang T, Secher NH. A reduced cerebral metabolic ratio in exercise reflects metabolism and not accumulation of lactate within the human brain. J Physiol. 2004;554(Pt 2):571–8.
122. van Hall G, Stromstad M, Rasmussen P, Jans O, Zaar M, Gam C, et al. Blood lactate is an important energy source for the human brain. J Cereb Blood Flow Metab. 2009;29(6):1121–9.
123. Quistorff B, Secher NH, Van Lieshout JJ. Lactate fuels the human brain during exercise. FASEB J. 2008;22(10):3443–9.
124. Rasmussen P, Nyberg N, Jaroszewski JW, Krogh-Madsen R, Secher NH, Quistorff B. Brain nonoxidative carbohydrate consumption is not explained by export of an unknown carbon source: evaluation of the arterial and jugular venous metabolome. J Cereb Blood Flow Metab. 2010;30(6):1240–6.
125. Dienel GA, Rothman DL. Glycogenolysis in cerebral cortex during sensory stimulation, acute hypoglycemia, and exercise: impact on astrocytic energetics, aerobic glycolysis, and astrocyte-neuron interactions. Adv Neurobiol. 2019;23:209–67.

126. Dienel GA, Cruz NF. Exchange-mediated dilution of brain lactate specific activity: implications for the origin of glutamate dilution and the contributions of glutamine dilution and other pathways. J Neurochem. 2009;109(Suppl 1):30–7.
127. Diaz-Garcia CM, Yellen G. Neurons rely on glucose rather than astrocytic lactate during stimulation. J Neurosci Res. 2019;97 883–9
128. Diaz-Garcia CM, Mongeon R, Lahmann C, Koveal D, Zucker H, Yellen G. Neuronal stimulation triggers neuronal glycolysis and not lactate uptake. Cell Metab. 2017;26(2):361–74 e4.
129. DiNuzzo M, Dienel GA, Behar KL, Petroff OA, Benveniste H, Hyder F, et al. Neurovascular coupling is optimized to compensate for the increase in proton production from nonoxidative glycolysis and glycogenolysis during brain activation and maintain homeostasis of pH, pCO(2), and pO(2). J Neurochem. 2024;168(5):632–62.
130. Chowdhury GMI, Jiang L, Rothman DL, Behar KL. The contribution of ketone bodies to basal and activity-dependent neuronal oxidation in vivo. J Cereb Blood Flow Metab. 2014;34(7):1233–42.
131. Overgaard Wichmann T, Hedegaard Højsager M, Hasager DH. Water channels in the brain and spinal cord—overview of the role of aquaporins in traumatic brain injury and traumatic spinal cord injury. Front Cell Neurosci. 2024;18:1414662.
132. Hladky SB, Barrand MA. Fluid and ion transfer across the blood-brain and blood-cerebrospinal fluid barriers; a comparative account of mechanisms and roles. Fluids Barriers CNS. 2016;13(1):19.
133. Vannucci SJ, Clark RR, Koehler-Stec E, Li K, Smith CB, Davies P, et al. Glucose transporter expression in brain: relationship to cerebral glucose utilization. Dev Neurosci. 1998;20(4–5):369–79.
134. Zeuthen T. Molecular water pumps. Rev Physiol Biochem Pharmacol. 2000;141:97–151.
135. Fischbarg J, Kuang KY, Vera JC, Arant S, Silverstein SC, Loike J, et al. Glucose transporters serve as water channels. Proc Natl Acad Sci USA. 1990;87(8):3244–7.
136. Fischbarg J, Kuang KY, Hirsch J, Lecuona S, Rogozinski L, Silverstein SC, et al. Evidence that the glucose transporter serves as a water channel in J774 macrophages. Proc Natl Acad Sci USA. 1989;86(21):8397–401.
137. Tomioka S, Kaneko M, Nakajo N. Pentobarbital inhibits glucose uptake, but not water transport by glucose transporter type 3. NeuroReport. 2012;23(11):687–91.
138. Tomioka S. Water transport by glucose transporter type 3 expressed in Xenopus oocytes. NeuroReport. 2012;23(1):21–5.
139. Duelli R, Maurer MH, Staudt R, Sokoloff L, Kuschinsky W. Correlation between local glucose transporter densities and local 3-O-methylglucose transport in rat brain. Neurosci Lett. 2001;310(2–3):101–4.
140. Duelli R, Kuschinsky W. Brain glucose transporters: relationship to local energy demand. News Physiol Sci. 2001;16:71–6.
141. Zeller K, Rahner-Welsch S, Kuschinsky W. Distribution of Glut1 glucose transporters in different brain structures compared to glucose utilization and capillary density of adult rat brains. J Cereb Blood Flow Metab. 1997;17(2):204–9.
142. Öz G, Berkich DA, Henry PG, Xu Y, LaNoue K, Hutson SM, et al. Neuroglial metabolism in the awake rat brain: CO2 fixation increases with brain activity. J Neurosci. 2004;24(50):11273–9.
143. Dienel GA. Stop the rot. Enzyme inactivation at brain harvest prevents artifacts: a guide for preservation of the in vivo concentrations of brain constituents. J Neurochem. 2021;158(5):1007–31.
144. Madsen PL, Schmidt JF, Holm S, Vorstrup S, Lassen NA, Wildschiødtz G. Cerebral oxygen metabolism and cerebral blood flow in man during light sleep (stage 2). Brain Res. 1991;557(1–2):217–20.
145. Madsen PL, Schmidt JF, Wildschiødtz G, Friberg L, Holm S, Vorstrup S, et al. Cerebral O2 metabolism and cerebral blood flow in humans during deep and rapid-eye-movement sleep. J Appl Physiol (1985). 1991;70(6):2597–601.
146. Madsen PL, Linde R, Hasselbalch SG, Paulson OB, Lassen NA. Activation-induced resetting of cerebral oxygen and glucose uptake in the rat. J Cereb Blood Flow Metab. 1998;18(7):742–8.
147. Linde R, Schmalbruch IK, Paulson OB, Madsen PL. The Kety-Schmidt technique for repeated measurements of global cerebral blood flow and metabolism in the conscious rat. Acta Physiol Scand. 1999;165(4):395–401.
148. Orzi F, Lucignani G, Dow-Edwards D, Namba H, Nehlig A, Patlak CS, et al. Local cerebral glucose utilization in controlled graded levels of hyperglycemia in the conscious rat. J Cereb Blood Flow Metab. 1988;8(3):346–56.
149. Hasselbalch SG, Madsen PL, Knudsen GM, Holm S, Paulson OB. Calculation of the FDG lumped constant by simultaneous measurements of global glucose and FDG metabolism in humans. J Cereb Blood Flow Metab. 1998;18(2):154–60.
150. Hyder F, Herman P, Bailey CJ, Moller A, Globinsky R, Fulbright RK, et al. Uniform distributions of glucose oxidation and oxygen extraction in gray matter of normal human brain: no evidence of regional differences of aerobic glycolysis. J Cereb Blood Flow Metab. 2016;36(5):903–16.
151. Herculano-Houzel S. The Remarkable, Yet Not Extraordinary, Human Brain as a Scaled-Up Primate Brain and Its Associated Cost. In: Striedter GF, Avise JC, Ayala FJ, editors. In the Light of Evolution: Volume VI: Brain and Behavior Washington D. C.: National Academies Press (USA); 2013.

Publisher's Note

Springer Nature remains neutral with regard to jurisdictional claims in published maps and institutional affiliations.